

Dark Matter in Cosmology

Litsa, Aliki¹, Bovenschen, Stan², and Heikamp, Marnix³

¹GRAPPA institute, University of Amsterdam, 11572418

²GRAPPA institute, University of Amsterdam, 10639578

³GRAPPA institute, University of Amsterdam, 11805188

June 29, 2018

Abstract

We review the role of dark matter in modern cosmology, including the various ways in which cosmological research can be used to strengthen the dark matter theory. We present the main astrophysical methods that have been used to solidify the dark matter theory over the last century. After a brief introduction to the basic cosmological concepts, we discuss various types of dark matter, as well as their main strengths and weaknesses. Furthermore, we explore the necessity of numerical simulations, which dominates the cosmological research and relates them to possible problems of the Λ CDM model. Lastly, we describe Modified Newtonian Dynamics (MOND) as an alternative explanation for the Universe in its present state, we conclude that this theory does not suffice for explaining certain properties of the universe.



Contents

1 Astrophysical methods in Dark Matter research (Aliki Litsa)	3
1.1 Velocity Dispersion	3
1.2 Rotation Curves	3
1.3 Gravitational Lensing	6
2 Cosmological Concepts (Aliki Litsa)	10
2.1 Recombination and the creation of the CMB (Aliki Litsa)	10
2.2 Inflation (Aliki Litsa)	10
2.3 CMB and the Baryon Acoustic Oscillations (Aliki Litsa)	11
2.4 Hubble measurements (Stan Bovenschen)	13
2.5 The Λ CDM model (Stan Bovenschen)	15
2.5.1 Latest measurements from the Planck telescope (Aliki Litsa)	15
3 Types of Dark Matter (Stan Bovenschen)	16
3.1 The possibility of baryonic dark matter (Marnix Heikamp)	16
3.2 Hot, Warm or Cold Dark Matter? (Stan Bovenschen)	16
3.2.1 Hot Dark Matter	16
3.2.2 Cold Dark Matter	17
3.2.3 Hot + Cold VS. Warm	17
4 Numerical Simulations in Dark Matter Cosmology (Aliki Litsa)	19
4.1 Excluding Hot Dark Matter with Numerical Simulations (Aliki Litsa)	21
4.2 Physics beyond the CDM model (Marnix Heikamp)	23
4.2.1 Problems on small scales	23
4.2.2 Mass of galaxies and dark matter halos	24
4.2.3 Considering baryonic matter	25
4.2.4 Numerical simulation	26
4.3 Effect of baryons on Numerical Simulations (Stan Bovenschen)	26
4.3.1 Baryonic matter in hydrodynamics	26
4.3.2 Numerical techniques	27
4.3.3 Modeling galaxies	28
4.3.4 Stellar streams	29
4.3.5 Future considerations (Marnix Heikamp)	29
4.4 Particle physics solutions (Marnix Heikamp)	30
4.4.1 Self-interacting dark matter (SIDM)	30
4.4.2 Fuzzy dark matter (FDM)	30
4.4.3 Warm dark matter (WDM)	30
5 Modified Newtonian Dynamics (Marnix Heikamp)	32
5.1 Milgrom's law	32
5.2 Conservation of momentum	32
5.3 MOND and the CMB	33
5.4 Gravitational waves	34
5.5 Bullet cluster	34

1 Astrophysical methods in Dark Matter research (Aliki Litsa)

The history of dark matter began in the 1930s, when a Dutch radio astronomer by the name of Jan Oort analyzed numbers and velocities of stars located close to our solar system and reached the conclusion that the particular stars appeared to be lacking approximately 30-50% of the matter necessary to account for their apparent velocities [1]. In 1933, and shortly after Oort's work, Fritz Zwicky performed similar calculations, and concluded that velocity dispersions in rich galaxy clusters require approximately 100 times more mass in order to ensure that they remain bound [2]. Similar research, including various other astrophysical and cosmological methods, continued more intensely during the following decades, and especially in the 1970s, when researchers attempted to further constrain the existence of such *invisible matter*, using galaxy rotation curves [3]. The following paragraphs contain an overview of the main astrophysical methods, which established the theory of dark matter in the minds of the scientific community.

1.1 Velocity Dispersion

As mentioned above, the earliest dark matter indications appeared through calculations related to the velocity dispersion of galaxies, and, in particular, those carried out by Zwicky on the Coma Cluster of galaxies [2]. In the particular paper, published in the 1930s, the velocities of galaxies belonging to the cluster were mentioned to differ by at least $1500 - 2000 \text{ km s}^{-1}$, according to various observations. Assuming that the Coma Cluster had reached a stationary state, Zwicky implemented the Virial Theorem as follows:

$$2E_k = -E_{pot},$$

where E_k and E_{pot} denote the average kinetic and potential energy per unit mass in the system. The cluster size was approximated by $R \sim 10^{24} \text{ cm}$, while including a total number of around 800 nebulae, each with a mass of $M_n \sim 10^9 M_\odot$. The additional assumption of uniform mass distribution for the contents of the cluster, yields a total cluster mass of $M_{CC} \sim 800 \times M_n \sim 1.6 \times 10^{45} \text{ gr}$. The potential energy of such a cluster is given by: $V = -\frac{3GM^2}{5R}$, resulting in an average potential energy per unit mass equal to $E_{pot} = -\frac{3GM}{5R} \sim -64 \times 10^{12} \text{ cm}^2 \text{s}^{-2}$.

In addition, the average kinetic energy can be expressed as $E_k = \frac{1}{2}\bar{v}^2 \sim 32 \times 10^{12} \text{ cm}^2 \text{s}^{-2}$. Using the expression of the virial theorem written above, the final result is:

$$(\bar{v}^2)^{1/2} \sim 80 \text{ kms}^{-1}.$$

Such a velocity appears to be very small compared to the Doppler effects of at least 1000 km s^{-1} measured from observations of the Coma Cluster. The ultimate conclusion that was drawn from the above was that the average density of the cluster, had to satisfy $\langle \rho \rangle \sim 400\rho_{lum}$. In other words, the real density had to exceed the density of the observed luminous matter by a factor of 400, in order for the cluster to remain bound. If the density failed to comply to this restriction, the 800 nebulae of the cluster would be bound to ultimately disperse and become independent of each other, thus no longer constituting a cluster of galaxies.

At this point, it is important to point out the fact that Zwicky's results, as mentioned above, were extremely preliminary, and failed to convince most members of the scientific community at the time. The main reason for that was that the calculation of redshifts for the galaxy-members of the Coma Cluster demanded the use of a Hubble constant which, in the 1930s, was very poorly constraint [4]. Furthermore, the uncertainties for the masses of the nebulae comprising the Coma Cluster weakened the argument for the difference between theoretically predicted and observed velocities even further. Whatever the inaccuracies, Zwicky's attempts constitute one of the first steps towards the exploration of the dark matter theory, and are, therefore, worth mentioning in our review. Similar calculations, making use of more accurate data, have, since, been performed for many more known large structures of matter in the Universe, since velocity dispersion constitutes one of the primary indicators for the existence of dark matter.

1.2 Rotation Curves

The rotation curve argument is another serious indication for the existence of dark matter in the Universe from the early years of research on the topic [3], until today [5, 6]. Such a curve is essentially a diagram of the rotational velocity versus the distance from the center of a galaxy, as presented in Figure 1. In this type of curves, rotation of stars dominates at smaller distances from the center of the galaxy, while gas rotation, studied through radio astronomy measurements, plays an important role at larger distances.

In the presence of *only* visible gravitational forces, simple Newtonian dynamics give:

$$\frac{Mv^2}{R} = \frac{GM^2}{R^2}$$

or

$$\frac{v^2}{R} = \frac{GM}{R^2}.$$

As a result, the *Keplerian rotation curve* follows the relation $v \propto R^{-1/2}$. However, the observations do not appear to agree with such a conclusion and, instead of rotation curves which decrease with the distance, they follow flat curves, indicating that the velocity has to satisfy $v \propto R^0$ instead. From the formula above one can find that $M \propto R$ when considering a constant velocity and, moreover:

$$\frac{dM}{dR} = \frac{v^2}{G}.$$

The essence of the argument used in order to reconcile observations with theoretical predictions supports that the Keplerian curves do, actually, accurately represent reality, but at much larger distances than the ones we are able to observe. Therefore, a logical conclusion indicates the existence of much larger galaxies, where great quantities of dark matter extend far beyond the visible matter, in what can be approximated as a spherically symmetric dark matter halo. The density of such a galaxy can be calculated from:

$$\rho = \frac{1}{4\pi R^2} \frac{dM}{dR} = \frac{v^2}{4\pi G R^2}$$

and, therefore, $\rho \propto R^{-2}$ beyond the visible radius.

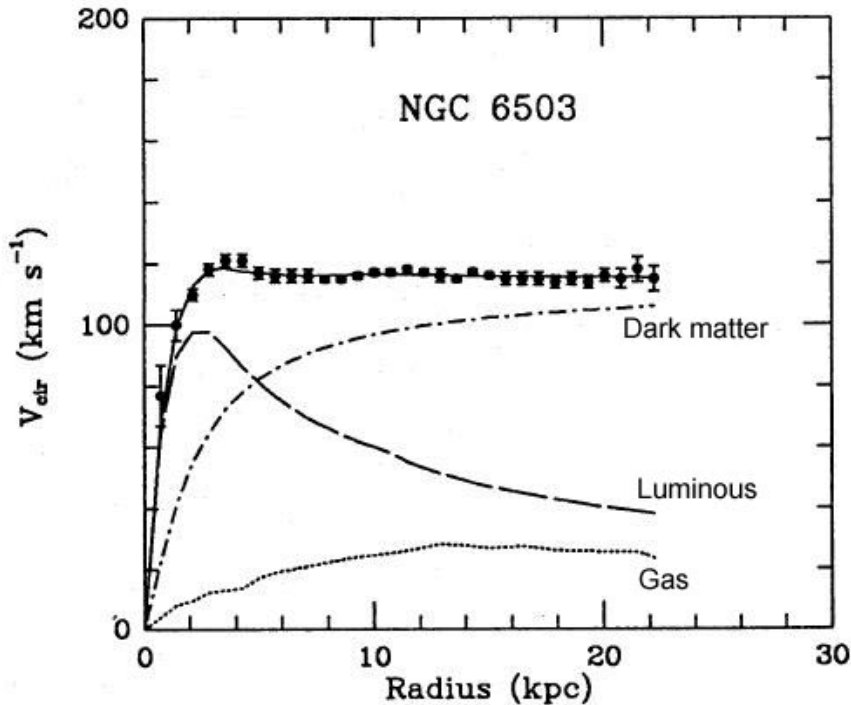


Figure 1: Rotation curve of NGC 6503 [7].

Having given the basis of the rotation curve argument in dark matter research, it is important to focus on some more recent results in relation to the same topic. One important paper to consider is that of McGaugh et al. (2016), which goes one step further in understanding the effect of galactic rotation [8]. The top panels of Figure 2 present rotation curves for three different types of galaxies, while the bottom panels depict the observed radial acceleration with respect to the radial acceleration in the case of a galaxy consisting of baryonic matter only. In those same bottom panels, the black lines refer to the actual relation between the two types of accelerations calculated, while the dashed lines correspond to the acceleration relation we would

expect for a galaxy consisting only of baryons. As expected, the baryonic approximation becomes accurate for larger acceleration values, which correspond to smaller radii, and, therefore, to distances from the center of the galaxy where baryons overpower dark matter. On the other hand, in the regime of small accelerations, which probe the actual dark matter halo, baryons can no longer play a significant role, and the two lines drift apart. From the figure it is, also, straightforward to conclude that, as galaxies get more and more faint (with the gas-dominated dwarf being the faintest), the observed acceleration reaches smaller and smaller values, which indicates that dark matter overpowers the galactic compositions. A result like that is justified, since a galaxy which is fainter has to include less luminous/baryonic matter.

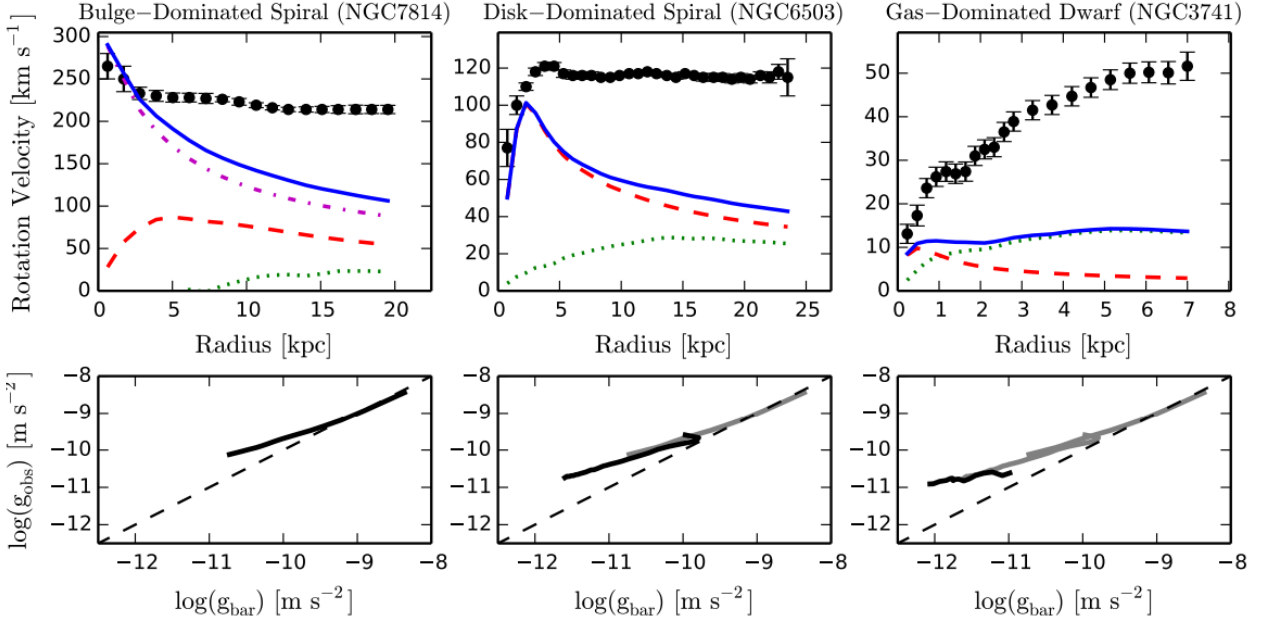


Figure 2: Top panels: Rotation Curves of individual galaxies. Each baryonic component is represented: dotted lines for the gas, dashed lines for the stellar disk, and dash-dotted lines for the bulge, when present. The sum of these components is the baryonic mass model (solid line). Bottom panels: Relation of observed radial acceleration to baryon radial acceleration. The solid lines represent the actual relation, while the dashed lines correspond to unity. From left to right each line is replotted in gray to illustrate how progressively fainter galaxies probe progressively lower regimes of acceleration. [8]

Another significant result of the particular paper is presented in figure 3, where the relation of the observed radial acceleration (from rotation curves) and the baryonic acceleration (from the solution of the Poisson equation) is plotted for 153 different galaxies. The resulting diagram indicates an extremely significant correlation between the two values, whose physical causes have yet to be explained with absolute certainty. A very intriguing fact worth mentioning is that the line created by the data points is predicted by expanded modified Newtonian dynamics theories [9] - the counter-argument to dark matter - which will be explained more thoroughly in section 5. Another possible explanation lies in small-scale structure formation, and indicates that it is the specific initial conditions of this procedure that have been imprinted on all galaxies which have arisen from it, thus interconnecting their properties. But are numerical simulations (see more in section 4) able to correctly reproduce the observational data and help us reach a conclusion on the physical cause of the correlation? As we can see in Figure 3, simulations create a dispersion around the correlation line due to the very large number of free parameters used, while observations place the galaxies exactly on it. As a result, one of the big concerns expressed by observational astronomers is the inability of simulated galaxies to accurately resemble the observed ones, and, thus, lead to trustworthy conclusions. According to McGaugh et al., the extent of the particular dispersion lies well within the expected error window, a fact which makes us optimistic with respect to the credibility of the dark matter theory. Whatever the true cause of the particular discovery, and the extend to which numerical techniques are sufficiently accurate, such a correlation constitutes an important finding, and an interesting argument for future research on the topic.

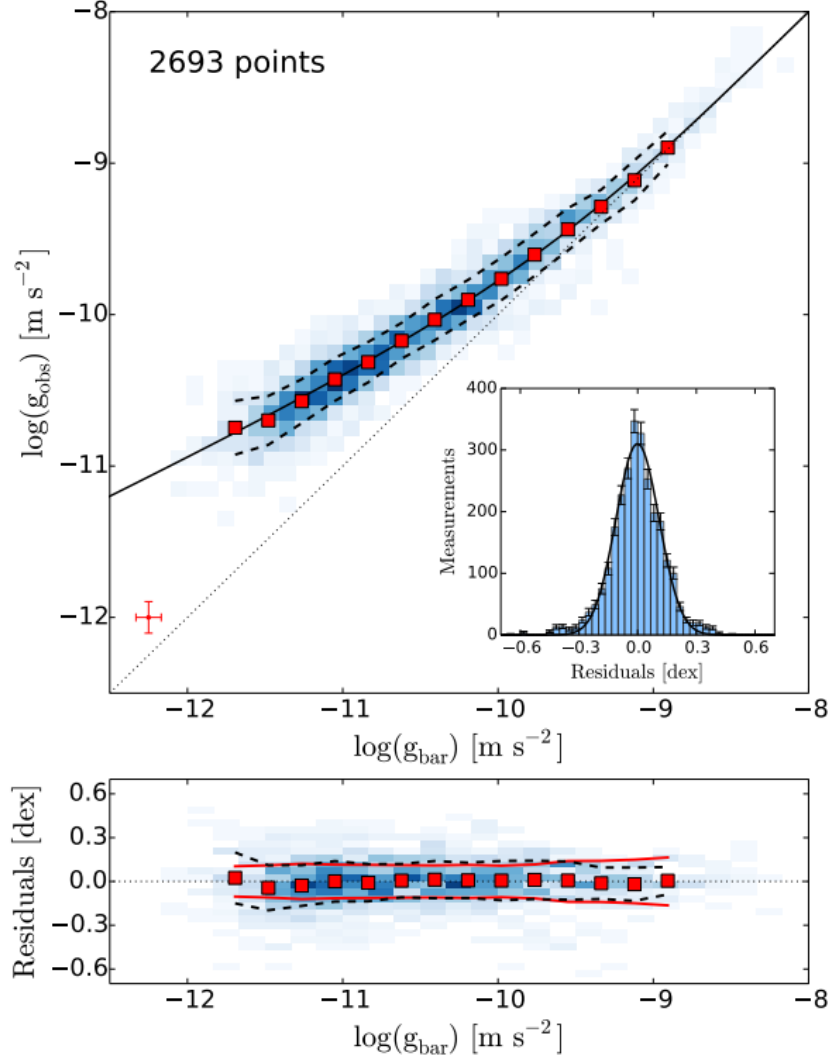


Figure 3: The centripetal acceleration observed in rotation curves, $g_{\text{obs}} = V^2/R$, is plotted against that predicted for the observed distribution of baryons, g_{bar} in the upper panel. Nearly 2700 individual data points for 153 SPARC galaxies are shown in grayscale [8].

1.3 Gravitational Lensing

Another astrophysical method that has been of paramount importance for the establishment of the dark matter argument is that of gravitational lensing, and especially of the weak gravitational lensing. More specifically, gravitational lensing is one of the various predictions made in Albert Einstein's theory of General Relativity and refers to the deflection of light by gravitational fields, as well as to the resulting effect of that deflection on images seen by an observer. In Figure 7 we can see a simple depiction of the gravitational lensing effect, in the case of light rays travelling from a distant quasar and being deflected by a galaxy-lens. The result is the creation of two *false images* of the quasar, which are observed from Earth, and give a false perception of the position of the quasar object on the celestial sphere. In Figure 4, we, also, present an example of strong gravitational lensing from Abell S295, where the two *false* images can, also, be observed very clearly.

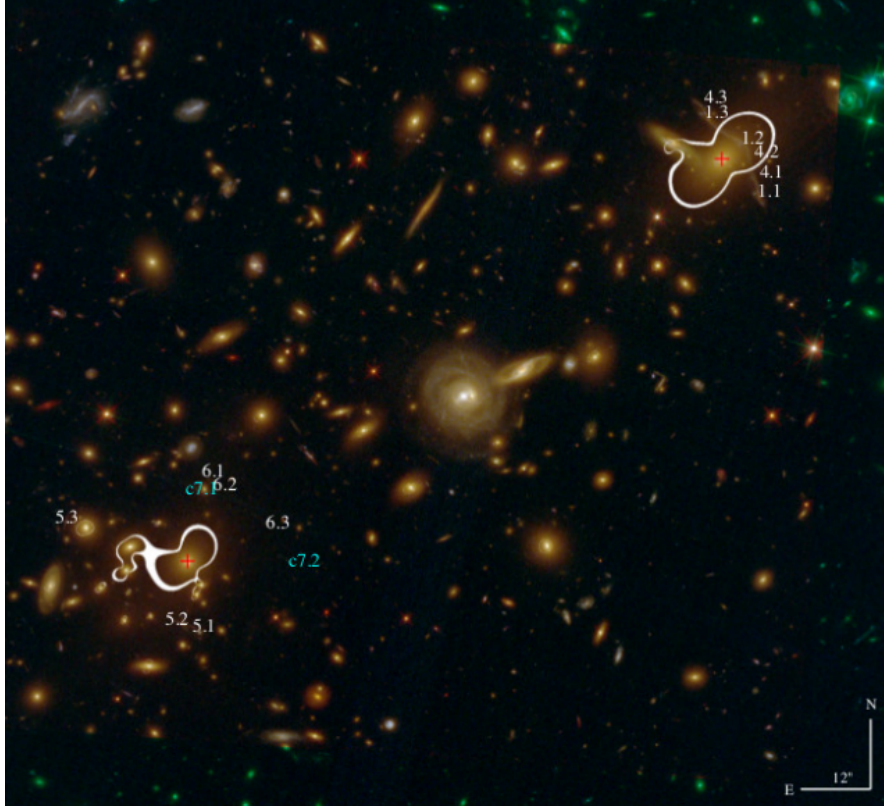


Figure 4: Strong gravitational lensing in Abell S295 [10].

There exist various types of gravitational lensing, depending on the strength of the effect and on the corresponding degree of image distortion of distant objects, including strong gravitational lensing, weak gravitational lensing and gravitational micro-lensing. More specifically:

- **Strong gravitational lensing**, in which case the mass of the lens is enough to produce multiple images, arcs, or even Einstein rings. Generally, the strong lensing effect requires the projected lens mass density greater than a critical density Σ_{cr} . For point-like background sources, there will be multiple images; for extended background emissions, there can be arcs or rings.
- **Weak gravitational lensing**, in which case the mass acting as a lens causes disfigurements to the background objects that are observed, but is not strong enough to produce arcs or rings. The particular type of lensing is used for the creation of *weak gravitational lensing maps* [11] like the one shown in Figure 5, which provide scientists with the opportunity of determining the mass distribution of distant massive objects. The comparison of such maps with actual observations of the luminous matter inside such objects can help determine the location of the dark matter component they consist of.
- **Gravitational microlensing**, in which case the lens allows the observation of sources producing little or no light, due to the collection and beaming of emitted light towards the direction of the observer.

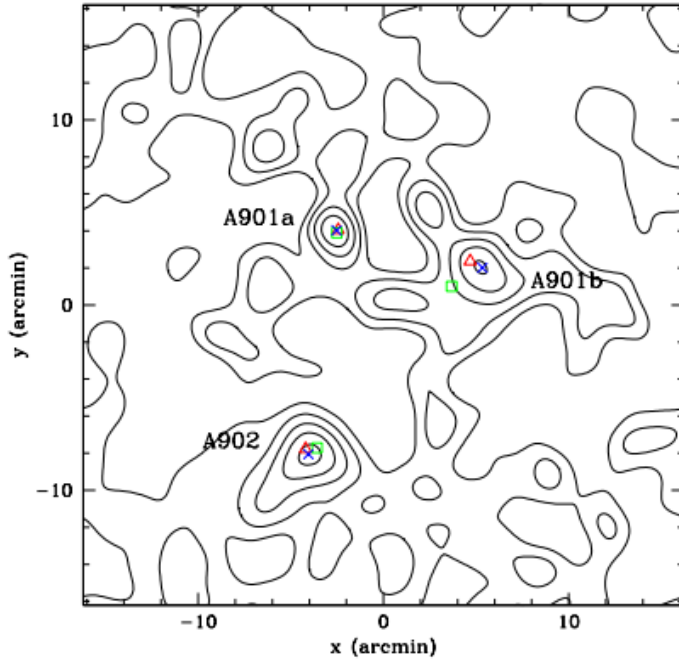


Figure 5: Two-dimensional projected distribution of mass in the A901/2 field. The contours show the lensing mass map of Gray et al. (2002) [12], with crosses, squares and triangles marking the location of the peaks in the mass and light distributions and the positions of the brightest cluster galaxies, respectively. [13]

In order to better understand the concept of gravitational lensing, we will attempt to present the simple basis of the argument using Einstein's theory of General Relativity, with light originating from a point-like source. The deflection angle α can be calculated from:

$$\vec{\alpha} = \frac{4GM}{c^2 b},$$

where b is the distance from the point-like source of the beam to the observer.

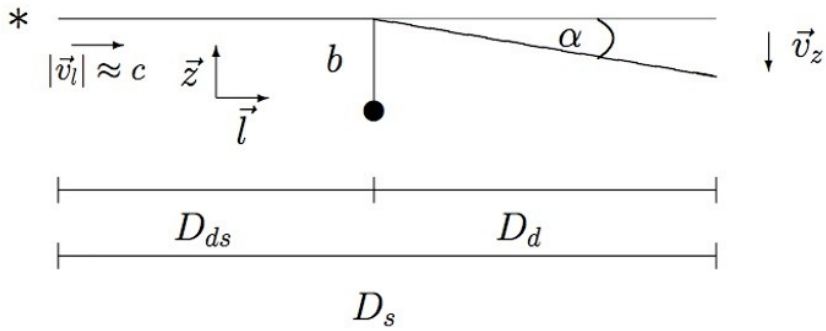


Figure 6: Deflection of a light beam originating from a point-like source.

If we consider the gravitational field as an optical medium with an index of refraction $n > 1$, the particular index is such that the light beam travels slower through the medium than through vacuum, and is given by [14]:

$$n = 1 - \frac{2}{c^2} \Phi = 1 + \frac{2}{c^2} |\Phi|,$$

where Φ refers to the gravitational potential. Furthermore:

$$\vec{\alpha} = - \int \nabla \perp n dl = \frac{2}{c^2} \int \nabla \perp \Phi dl$$

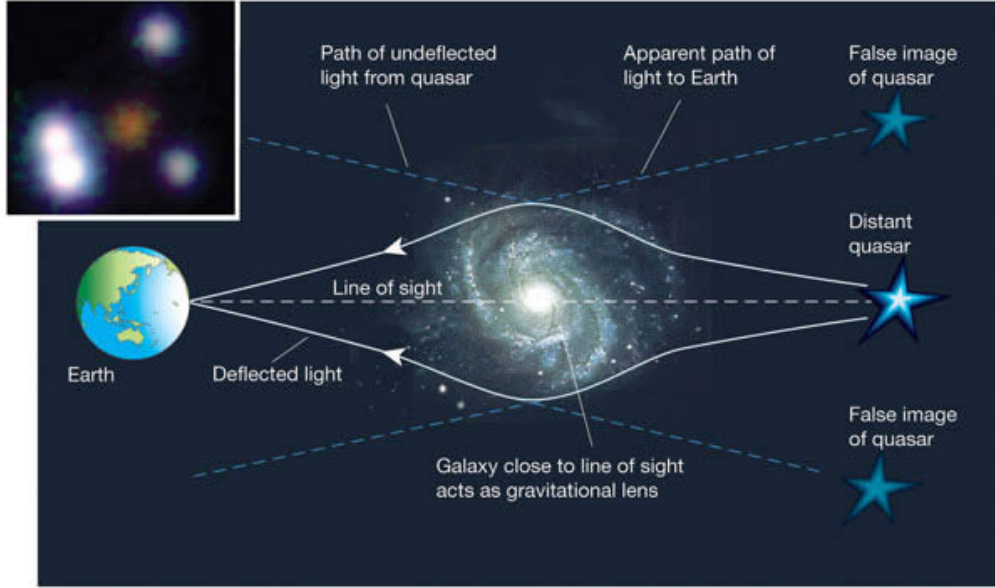


Figure 7: Lensing effect (taken from <https://pics-about-space.com/gravitational-lensing-and-dark-matter>).

which contains the integral of the potential gradient perpendicular to the light propagation direction ($\nabla \perp \Phi = \frac{d\Phi}{dz}$). Therefore, for a light beam traveling at a distance $b = R_{\text{sun}}$ from the center of the Sun (which is considered as a point-like source), the deflection angle α is calculated to be approximately $1.7''$. Further topics that are related to gravitational lensing include the lens equation, as well as the phenomenon that is known as the Einstein ring. However, such discussion goes beyond the purposes of the particular review.

The method of gravitational lensing can also be applied in *Bullet Cluster* observations, where two clusters are undergoing high-velocity collisions and subsequently emit X-rays that have been detected by the Chandra telescope. The interested reader can find out more by reading [15, 16, 17]. In images of such phenomena that have been captured we can observe two different types of material. The *hot gas* is concentrated at the collision front, while some dark matter, confirmed by weak gravitational lensing techniques, is concentrated behind the collision front (as can be seen in Figure 8). We can, therefore, conclude that the dark matter detected in such phenomena, not only exists, but is also collisionless.



Figure 8: Bullet Cluster 1E0657-558. Blue refers to the collisionless dark matter and red to the hot baryonic matter in the collision front. Image provided courtesy of Chandra X-ray Observatory. [18]

2 Cosmological Concepts (Aliki Litsa)

A deeper understanding of dark matter physics requires a good understanding of the cosmological concepts of inflation, as well as those of baryon acoustic oscillations and the Cosmic Microwave Background (CMB). The following paragraphs contain a brief overview of the knowledge necessary for the understanding of the topics presented in this review.

2.1 Recombination and the creation of the CMB (Aliki Litsa)

The history of the Universe begins at time $t = 0$ with the Big Bang, and continues until today ($t \sim 10^{10}$ yr). During the early stages of cosmological evolution, the Universe was hot and dense, and consisted of an ionized plasma, where baryonic matter and radiation were strongly coupled together. While the temperature of the Universe exceeded the value of $\sim 4 \times 10^3$ K, the formation of neutral atoms from electrons and protons was impossible due to the extremely high energies of the plasma, which surpassed the hydrogen binding energy. Under such circumstances, the electron number density remained very high and, due to the continuous electron-photon interactions via Thomson scattering, limited the mean free path of photons considerably, thus keeping them from travelling independently of the matter component.

When the age of the Universe reached 377,000 years the temperature dropped below 4×10^3 K and, as a result, electrons joined protons in order to create neutral atoms. The particular phenomenon is known as *recombination*, and resulted in a significant drop of the electron number density, allowing photons to escape the plasma and travel freely in the Universe. The same radiation, which was released during this *photon decoupling*, is still measured today at a temperature of ~ 2.7 K and is known as the CMB. A picture of the CMB as measured by the Planck telescope is shown in Figure 9.

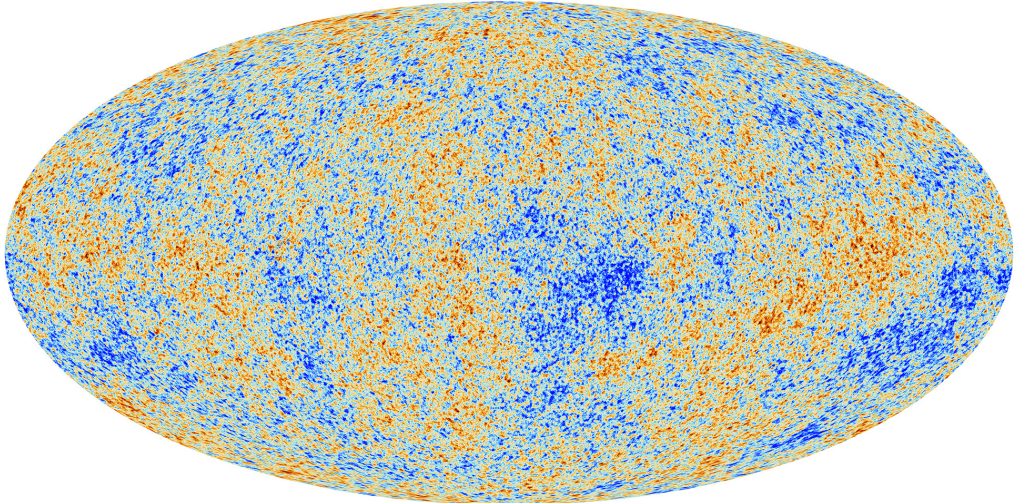


Figure 9: The anisotropies of the CMB radiation as measured by Planck. Taken from: <https://www.esa.int>.

2.2 Inflation (Aliki Litsa)

Another important concept, which is necessary for the understanding of the transformation of the Universe into its current form, is that of the inflation mechanism. The need for inflation is reflected in the following paragraphs.

According to measurements of the CMB radiation made by the Planck telescope and its predecessors, the Universe appears to be homogeneous and isotropic on large scales, up to a factor of 10^{-5} [19]. Such a uniformity can only be achieved if the furthest regions of the Universe have already been in causal contact in the past. More specifically, such a uniformity indicates that light must have been able to travel across all these uniform regions in the past, thus smoothing out any prominent inhomogeneities. Such a causal contact cannot be explained by the basic cosmological theory and gives rise to what is known as the horizon problem. Figure 10 presents the horizon as seen by an observer today (at point A) looking towards the time of decoupling. Observers B and C exist at the time of decoupling and have independent horizons that do not intersect with each other, thus containing regions which are not in causal contact. Despite the fact that the regions seen by observers B and C at the time of the CMB release appear to be entirely detached from each other, observer A witnesses a CMB which is extremely uniform.

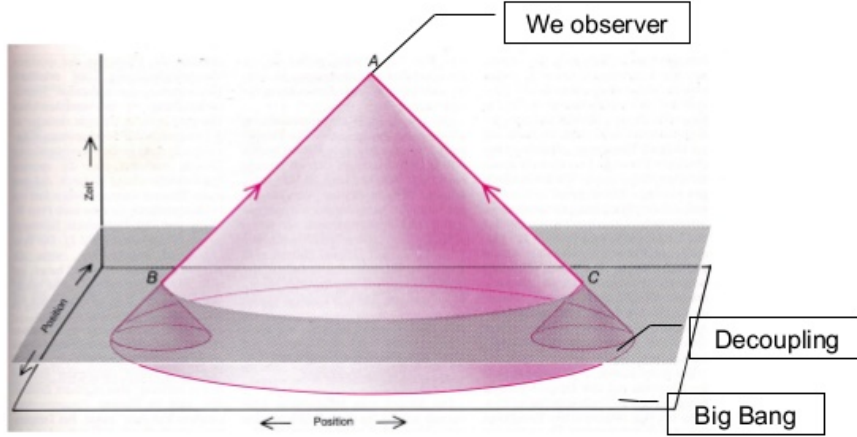


Figure 10: The horizon problem.

The solution to the problem is given by the inflation mechanism [20, 21], which provides an exponential expansion of the Universe at negative conformal time, even before the Big Bang event. According to the inflation scenario, all regions were in causal contact, inside the Hubble sphere at some point in the past. However, due to such an accelerated expansion many regions exited the Hubble sphere (the *causal contact sphere*), and thus appeared causally disconnected at the time of the Big Bang and of recombination.

However, the "blessings" of the inflation mechanism are not restricted to the solution of the horizon problem. The Planck telescope and its predecessors have measured a Universe which is very close to perfectly flat. Such a result indicates that the Universe had to be even flatter in the past, a fact which can only be explained by a theory of accelerated expansion [22]. The mechanism of inflation takes the flat counterparts of a curved Universe and, through intense expansion, amplifies them to such an extent that the observable Universe appears very close to perfectly flat today. Furthermore, inflation is able to produce the very precise initial conditions necessary for structure formation to take place and result in the creation of the Universe as observed today (more on structure formation in section 4). It, therefore, solves the *fine-tuning* problem, and provides the seed for large-scale structure formation in the form of adiabatic density perturbations [23].

2.3 CMB and the Baryon Acoustic Oscillations (Aliki Litsa)

Having already mentioned various astrophysical methods of establishing the credibility of the dark matter argument in section 1, it is time to move on to some cosmological phenomena. The Baryon Acoustic Oscillations are those that give rise to the various acoustic peaks in the Cosmic Microwave Background power-spectrum, as well as in the matter power-spectrum and are, therefore, imprinted on the large-scale structure in galaxy surveys [24]. Their creation took place in the Early Universe, before the recombination of electrons and protons for the formation of neutral hydrogen atoms and the subsequent release of the CMB radiation. During this early age of the Universe, the various cosmological perturbations caused the excitation of sound waves in the relativistic plasma. The particular sound waves resulted in the oscillation of modes, which arose from the constant "struggle" between the gravitational potential and the radiation pressure. Figure 11 depicts the particular "struggle", where the radiation pressure pushes the oscillating modes out of the gravitational well, and the gravitational potential acts as a restoring force by dragging them back in. Until the time of recombination all the various modes of different wavelength had completed a different number of oscillation periods, a fact that has been "captured" in the CMB power spectrum as the different maxima and minima shown in Figure 12. While, however, the baryon perturbations travelled outwards in the form of an acoustic wave, the dark matter perturbations grew in place. At the time of recombination, the speed of sound fell rapidly, which resulted in the end of the sound-wave propagation, at a moment when the baryon acoustic shell had expanded to a radius of ~ 150 Mpc. It is after the time of recombination, at redshift $z \sim 1100$, that dark matter perturbations, along with the baryonic perturbations contribute to the creation of all large-scale structures observed in the Universe today. If dark matter failed to exist, and its corresponding perturbations failed to dominate over the baryonic acoustic perturbations, the resulting structures created would significantly differ from the Universe as we observe it today.

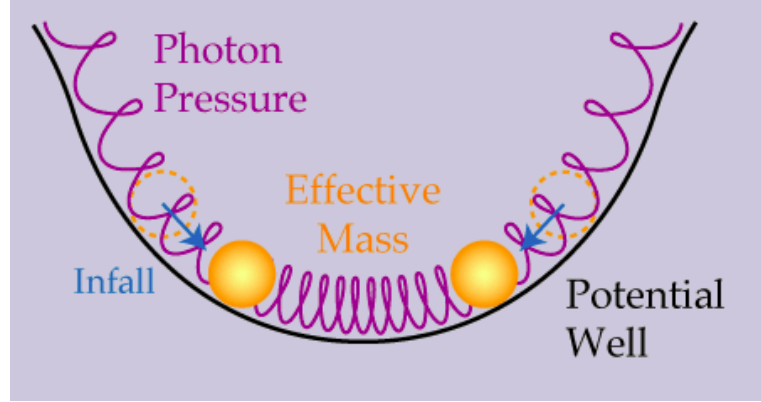


Figure 11: Baryon Acoustic Oscillations: the gravitational potential drags modes inside the well, while the radiation pressure pushes them out. Taken from: <http://background.uchicago.edu/whu/physics/acoustic.html>.

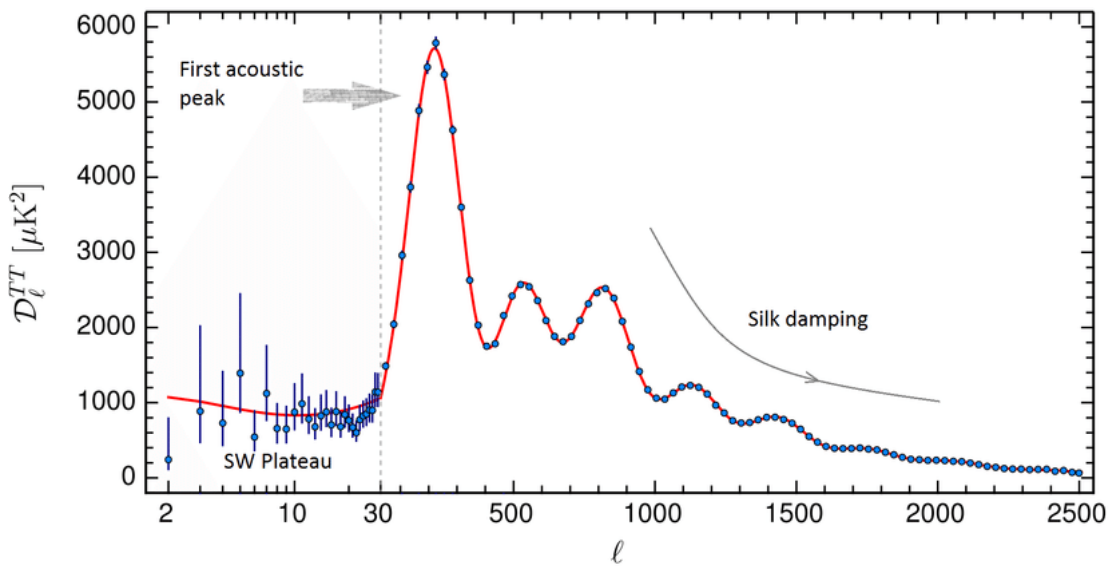


Figure 12: The CMB anisotropy power spectrum found by the Planck collaboration [25].

Of all the peaks in the CMB anisotropy power spectrum, it is the third peak that can provide us with information related to the dark matter component in the Universe. More specifically, having a third peak with an amplitude that exceeds that of the second peak is a clear indication that dark matter dominated the matter density in the plasma before recombination. The particular peak of the CMB power spectrum corresponds to modes that have completed more oscillations compared to the first two peaks, or, in other words, have began oscillating earlier on, during the radiation domination era. During the particular era, radiation pressure dominates compared to the gravitational potential, and the potential decays, driving the oscillation amplitude of baryons up (known as the *driving effect*). Since this driving effect of radiation domination cannot have a large influence when the Universe becomes matter dominated and the gravitational potential is significant, the second peak does not experience a similar rise in amplitude. Furthermore, during matter domination, dark matter contributes to the gravitational potential, which is no longer decayed, thus reducing the baryonic acoustic oscillation amplitude. As a result, depending on the dark matter energy density, the third peak, which corresponds to radiation domination, is expected to overpower the second, which captures oscillations in the matter - and, therefore, dark matter - domination period. We can, therefore, estimate the dark matter energy density based solely on CMB observations, and confirm the existence of an additional component, apart from regular (baryonic) matter itself, that is essential in accounting for the cosmological structure witnessed. Such a conclusion provides a strong ally of the dark matter argument, from a cosmological perspective.

At this point it is important to point out another very interesting fact about baryon acoustic oscillations. We have, already, explained how these baryon oscillations are imprinted on the CMB anisotropy power spectrum shown above, as all the different maxima and minima observed. Another very significant effect of

these oscillations is that they are, also, imprinted on the late-time power spectrum $P(k)$ of the non-relativistic matter in the Universe [26, 27, 28, 29], at the exact positions corresponding to the oscillation peaks in the CMB anisotropy power spectrum. The matter power spectrum, as shown in Figure 13, corresponds to the matter perturbation squared and is calculated by: $P_\Delta(k, z) = |\Delta_{m,k}(z)|^2$. We can therefore observe how the baryon acoustic oscillations, not only have affected the temperature fluctuations found in the CMB, but also the layout of the matter component in the Universe itself. Such a notion appears to be reasonable, since an oscillation of baryonic matter is bound to have an influence on the distribution of the particular matter.

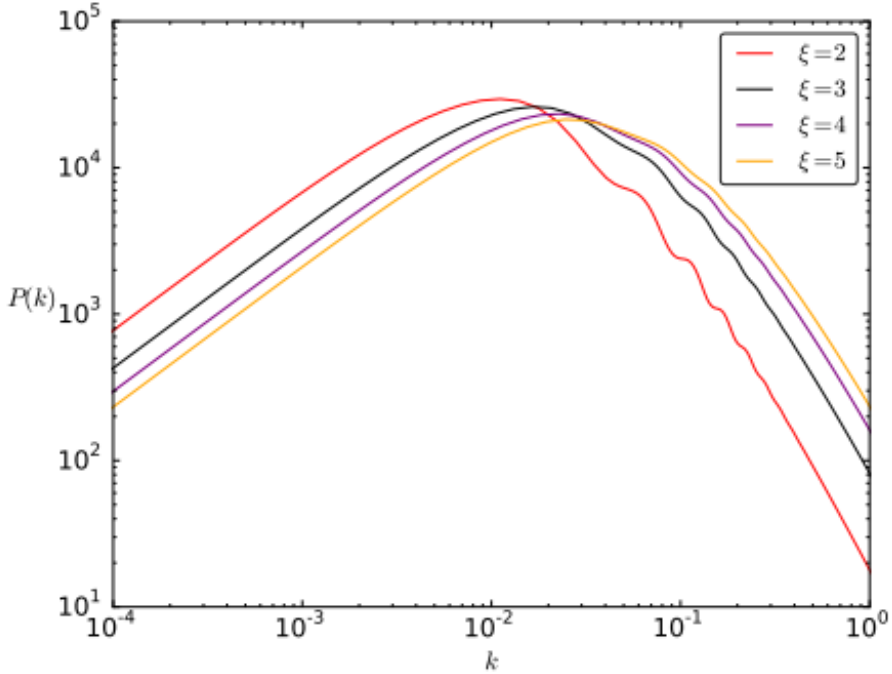


Figure 13: The matter power spectrum [30], where $\xi = 3$ corresponds to the Universe as we know it. Visible are small amplitude baryon acoustic oscillations in the spectrum.

2.4 Hubble measurements (Stan Bovenschen)

It is well known that the Hubble parameter measures how fast the Universe is expanding at a given age of the Universe. With the Hubble parameter today, the Hubble constant, we are able to make an estimate of the age of the Universe by calculating how long it took the Universe to expand to this point. The most common way of measuring the Hubble constant is by using supernovae Ia as standard candles. The magnitudes of supernovae type Ia are well known, so we can calculate the distances to them. Also, we know the redshift of the supernovae and we can thus calculate the Hubble constant. This method is a direct measurement in the local Universe. The most precise measurement today is [31]:

$$H_0^{local} = 73.24 \pm 1.74 \text{ km s}^{-1}\text{Mpc}^{-1}$$

Another method to measure the Hubble constant is an indirect way. This method uses observations of the CMB and large scale structures. The observations of the CMB powerspectrum from the Planck telescope are in agreement with the spatially flat Λ CDM model. The Hubble constant calculated from these observations are not consistent with the above mentioned local observations [19]:

$$H_0^{Planck} = 67.8 \pm 0.9 \text{ km s}^{-1}\text{Mpc}^{-1}$$

Of course, those values should be the same since the age of the universe is the same everywhere in space. The first thing to check are the systematic errors in either the CMB measurements or in the local measurements. This has been done extensively in the past few years. When the values got more precise the discrepancy did not disappear. The newly calculated local Hubble constant is still 3.1σ larger than the

Hubble constant from the updated Planck measurements [32]. Since the Planck values of the Hubble constant arise by assuming the Λ CDM model, an other possible explanation could be that the Λ CDM model is simply incorrect.

A potential solution could be found from considering the local Universe to be different from the global Universe. If the local Universe would have an underdensity, it could cause the local Hubble constant to be higher. A region with lower density expands faster, therefore it looks like the Universe is younger since it takes less time to expand to a certain volume. We know that the Hubble constant scales as $H_0 \propto \frac{1}{\tau_{universe}}$. Therefore H_0 would be higher in the local underdense Universe. This has been investigated using local inhomogeneities on the luminosity distance, which are caused by relativistic effects. It turns out that the radial profile has an underdensity of 300 Mpc h^{-1} in one direction [33]. This fluctuation in luminosity distance is related to the Hubble parameter by:

$$\frac{\Delta H(z)}{\bar{H}_0} = -\frac{\Delta D_L(z)}{\bar{D}_L(z)} = -\frac{1}{3}f\bar{\delta},$$

where $\bar{\delta}$ is the average density contrast over a co-moving sphere. In figure 14 this relation is shown. We clearly see an underdensity at $0.1 < z < 0.4$. This results in a higher Hubble parameter in this region. At higher z , we see no fluctuation anymore since the local underdensity is negligible on global scale.

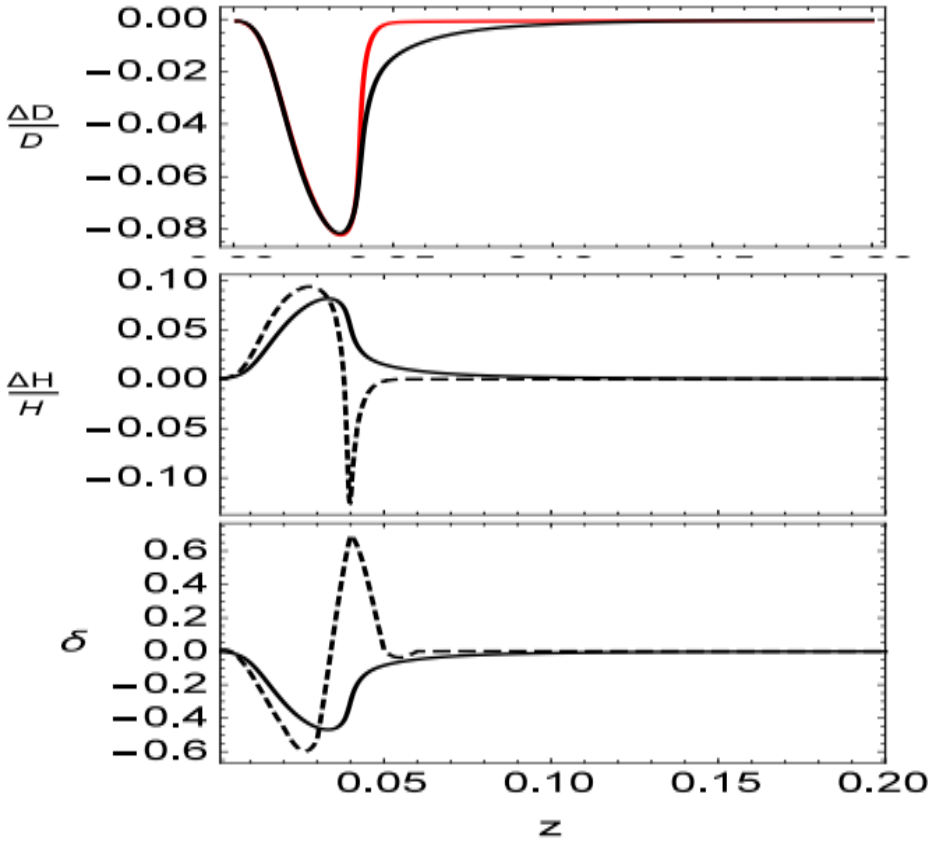


Figure 14: Relation between inhomogeneities in luminosity distance and inhomogeneities in values of the Hubble constant due to a local underdensity (top and middle panel respectively). Bottom panel: the density contrast over a co-moving sphere. The red line in the top panel is the luminosity distance calculated with a non-perturbative approach, this is in agreement with the black line. The dashed line is the Newtonian limit of the cosmological scalar perturbation theory [33].

Whether this application of the Λ CDM model can explain the total discrepancy of the Hubble constant remains unsolved [33]. Other approaches, based on perturbation theory or by using N-body simulations have also been investigated extensively. See [34] for a comparison between these two approaches.

2.5 The Λ CDM model (Stan Bovenschen)

Λ CDM is a model that combines the components of dark energy and cold dark matter, and the most plausible model of the Universe today. Cold dark matter is explained in section 3.2.2. In order to know what amount of dark matter and dark energy we are looking for we can measure the density parameter Ω :

$$\Omega = \frac{\rho}{\rho_c} = \frac{8\pi G\rho}{3H_0^2}$$

This parameter can be measured for every component in the universe, together the density parameters of all components should add up to one: $\Omega_{tot} = 1$. The different components of Ω are being measured by the Planck telescope, including Ω_Λ . The fact that we are measuring this component of the density parameter means that there is some dark energy in the Universe. Hence we have to use the Λ CDM model.

2.5.1 Latest measurements from the Planck telescope (Aliki Litsa)

The measurements made by the Planck telescope [25] are constraint using all astrophysical methods mentioned in section 1, as well as the Baryon Acoustic Oscillation information mentioned in section 2.3. Some additional constraints are calculated using distance and velocity measurements of Type Ia Supernovae - the "standard candles" of astrophysical observations - as explained in section 2.4. The total energy density of all components, considering a nearly flat Universe, is expected to be $\Omega_{tot} \sim 1$. According to measurements of the telescope made in 2015, the other components have the following characteristic values:

- Physical baryon density parameter: $\Omega_b h^2 \simeq 0.02230 \pm 0.00014$
- Physical dark matter density parameter: $\Omega_c h^2 \simeq 0.1188 \pm 0.0010$
- Dark energy density parameter: $\Omega_\Lambda \simeq 0.6911 \pm 0.0062$
- Hubble's constant at the present time: $H_0 \simeq 67.74 \pm 0.46 \text{ km s}^{-1} \text{ Mpc}^{-1}$
- Matter density parameter: $\Omega_m = \Omega_c + \Omega_b$: $\Omega_m \simeq 0.3089 \pm 0.0062$
- Critical density: $\rho_{crit} \simeq (8.62 \pm 0.12) \times 10^{-27} \text{ kg/m}^3$
- Age of the Universe: $t_0 \simeq (13.799 \pm 0.021) \times 10^9 \text{ yr}$
- Scalar spectral index: $n_s \simeq 0.9667 \pm 0.0040$
- Reionization optical depth: $\tau \simeq 0.066 \pm 0.012$
- Sum of three neutrino masses: $\Sigma m_\nu \simeq 0.06 \text{ eV}/c^2$
- Effective number of relativistic degrees of freedom: $N_{eff} \simeq 3.046$
- Redshift at decoupling: $z_* \simeq 1089.90 \pm 0.23$
- Age at decoupling: $t_* \simeq 377,700 \pm 3,200 \text{ yr}$

where $h = \frac{H_0}{100 \text{ km s}^{-1} \text{ Mpc}^{-1}}$ the reduced Hubble constant.

The values above constitute most of the essential characteristics of the Λ CDM model, while those of them related to the density parameters express the contribution of each of the components to the content of the Universe. Some of the problems of the particular model will be discussed in the following sections of the review.

3 Types of Dark Matter (Stan Bovenschen)

In the previous section we have seen several arguments towards the existence of dark matter. In the coming sections, we want to show this by exploring the ways in which dark matter could be found. To be able to start looking for dark matter we first have to know what to look for.

In this section, we will narrow down what dark matter is comprised of by explaining whether dark matter consists of baryons. We will also discuss some dark matter models from which we can extract the make-up of dark matter.

3.1 The possibility of baryonic dark matter (Marnix Heikamp)

We have readily seen that dark matter exist, though we have yet to determine what kind of matter dark matter consists of. There are various possibilities of matter to consider, some of which will be discussed below, along with the likelihood of dark matter to be composed of them.

The most straightforward thing to assume is that dark matter consists of ordinary baryons, that we haven't found yet, however there are several issues that arise:

- **The amount of baryons.** There exist two ways in which we can measure the amount of baryons that are present in the Universe. Firstly, we can measure the abundance of light elements, specifically deuterium from the ratio between the amount of photons and baryons that are present in our universe from BBN [35]. Secondly, we can consider the distribution of hot and cold spots in the CMB. Both of these turn out to be in excellent accordance with one another. As we saw, the energy density for baryonic matter is $\Omega_b = 0.02230/0.49 \approx 0.05$ (where h is taken to be 0.7, whereas the total energy density of all matter in the Universe is approximately 0.30). Thus, there not enough baryons exist to make up dark matter.
- **Various candidates are unlikely.**
 - **Hydrogen or helium gas.** When hydrogen is frozen, it forms 'snowballs' which would evaporate and thus do not contribute. When helium is in a cool state, it should absorb light that comes from behind it, but this is scarcely witnessed. When there's hot gas, this should emit X-ray radiation, but this is also scarce.
 - **Dusts, rocks or asteroids.** More complex elements may create bigger objects, such as rocks or asteroids. However, that would imply that stars should also have higher metallicity than is the case. This is thus not likely. For dust to be present, we should have more blocking of light, which is not abundant. So, also baryonic dust cannot be the constituent of dark matter.
 - **MACHOs [36].** MACHOs, very low luminosity stars are hard to witness, for apparent reasons. They can be found using gravitational microlensing. Although some have been found over the last decades, it does not nearly come close to explaining all the missing matter in the Universe.
 - **Very massive objects.** The remnants of very massive stars that formed early in Galactic history might form neutron stars and massive black holes. For neutron stars to form, a star usually goes supernova, ejecting many heavy elements into the Universe, which we don't observe. Additionally, the final mass of a neutron star is not high enough to explain all the missing matter. Very massive stars usually end their lives by collapsing into a black hole, which is unlikely to have happened enough to explain the amount of matter that is required.

3.2 Hot, Warm or Cold Dark Matter? (Stan Bovenschen)

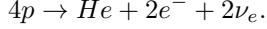
We have seen that dark matter cannot be baryonic nor weakly interacting. In addition to the types of dark matter explained in section 3.1 we can consider three different models for dark matter: hot, warm and cold dark matter.

The difference in these models comes from considering whether dark matter particles were relativistic just before recombination. This difference could have a big influence on the matter structures in later stages of the Universe. Therefore, we have to look closely at the CMB, which is a direct remnant of the recombination era, and at the density distribution of matter throughout the Universe.

3.2.1 Hot Dark Matter

Hot dark matter particles are relativistic just before recombination. Around 1980, the hot dark matter model was very popular, since neutrinos seemed to be a good candidate for hot dark matter [37]. People had just

found out about some unexpected characteristics of neutrinos [38]. Before this time, neutrinos were thought of as massless particles. This changed when the solar neutrino problem was encountered. More specifically, neutrinos are produced in the Sun by:



When neutrinos are measured on Earth, only 1/3 of the expected amount is found. The solution to this problem is that neutrinos oscillate, thus constantly changing flavor between ν_e , ν_μ and ν_τ . This is only possible if neutrinos have mass [39]. And thus, people thought neutrinos could be dark matter, since they are weakly interacting. However, hot dark matter requires small scale structures to be damped. The density perturbations in the primordial fluid are damped by the free-streaming, relativistic neutrinos. This causes the initial structures in the early Universe to be of size $\lambda_c = 41(m_\nu/30\text{eV})^{-1}$ Mpc, which is the typical distance a neutrino travels in the lifetime of the Universe. Smaller scales, like galaxies, would form later as a consequence of fragmentation [40]. We find that this is not the case in the Universe and we conclude that λ_c for hot dark matter is too large. [37]

Another way of answering the question whether dark matter in the form of neutrinos is possible is by looking at the density parameter, which indicates the dominant component of the Universe. Ω_ν is proportional to the total neutrino mass [41]:

$$\Omega_\nu h^2 = \frac{\sum m_\nu}{93\text{eV}}$$

As m_ν is tiny, Ω_ν must be small. Thus, when neutrinos were to be dark matter they would be dominated by the other components of Ω and would thus not play a big role in the creation of the Universe.

Still, neutrinos are very helpful in the realm of dark matter since they could be produced by dark matter annihilating in the galaxy. Neutrinos are the only particles produced by dark matter that could escape from the initial objects [42]. This implies that we can use neutrino telescopes to observe dark matter.

3.2.2 Cold Dark Matter

As said before, λ_c for hot dark matter is too large. Alternatively to this hot dark matter, a cold dark matter model has been studied extensively. In this model we do not encounter this particular problem. In CDM, dark matter was non-relativistic before recombination. This causes matter fluctuations to be only growing during the radiation era if their wavelengths are larger than the horizon scale [37]. After that, during the matter dominated era, all fluctuations are growing with the same rate. In this way, large scale structures can arise [37], as mentioned in section 2.3. There are many cold dark matter candidates, the most prominent of which are weakly interacting massive particles (WIMPs) and axions, each with different properties.

For WIMPs, it is needless to say that they are weakly interacting (otherwise we could observe them easily) and massive (they need to solve the observed lack of mass). In addition to these obvious properties, they can produce neutrinos, photons, electrons and protons. The latter two can produce more high energy photons through inverse Compton scattering. As a result, the CMB could possibly be upscattered by these electrons [42].

Axions are designed to solve the strong CP-problem. Initially the CP-symmetry was supposedly not being violated, until researchers realized that the weak interactions did indeed violate the symmetry [43]. However, it is not known whether the CP-symmetry should be violated for the strong interactions. Experimental research has not been able to give reliable proof of such a violation [44]. However, there is no reason for it to be conserved, which has led physicists to ask the question as to why it is being conserved. Violation of CP-symmetry causes the axion to have a mass. Both the mass and the strength of the interactions is extremely small, which fits with the predictions of dark matter [45].

Unfortunately, the cold dark matter model also brings some complications with it. While on large scales everything appears to be fine, things on smaller scales are not entirely correct. Galactic velocities on small structures are too large and there are too many clusters of galaxies [46]. In order to correct for those unwanted properties there are two additional dark matter models: the hot + cold dark matter model and the warm dark matter model, both discussed in section 3.2.3. Nowadays the Λ cold dark matter (Λ CDM) model, as discussed in section 2.5, is seen as the most plausible model for dark matter.

3.2.3 Hot + Cold VS. Warm

Previously in this section we have seen that the hot and the cold dark matter model both have flaws. Hot dark matter erases the small scales in the early Universe. Cold dark matter, on the other hand, predicts too many clusters of galaxies, and the galactic velocities on small scales are too large. The obvious combination

of the two is the hot+cold dark matter model. This model tries to find the right ratio between cold and hot. In 1993, the following values seemed to agree very well with the observations at that time [47]:

$$\Omega_{cold} = 0.6, \quad \Omega_\nu = 0.3, \quad \Omega_{baryon} = 0.1$$

$$H_0 = 50 \quad km \cdot s^{-1} \cdot Mpc^{-1}$$

where the hot dark matter candidate is considered to be the neutrino. The density parameter Ω_ν , gives a total neutrino mass of $m_\nu = 7eV$. Despite the agreement with most observations there are a few exceptions: With the given neutrino mass, galaxies may not be able to account for observations of quasars and damped Ly- α systems at high redshift because they form too late. To tune the results a little further, the total neutrino mass in the cold+hot dark matter model has to be lowered from $7eV$ to $\sim 5eV$ [46]. Because the neutrino oscillation's were not quite well understood at the time, the total neutrino mass was split up into the tau and muon neutrino masses:

$$m_\tau \approx m_\mu \approx 2.4eV$$

This way the calculations for large, astronomical, scales seemed to fit quite well. On the other hand, in the particle physicists point of view, the hot + cold dark matter model was less appreciated, since the calculated masses where too high to be neutrinos [40].

This problem can be fixed by introducing a hypothetical particle, the sterile neutrino, which could be a form of warm dark matter. Warm dark matter particles have an even lower cross section than neutrinos and are less abundant. They have a mass of $\sim 1keV$. In this case λ_ν is much lower [40]. Warm dark matter is not yet excluded from being a possible model for dark matter, though some issues are discussed in section 4.4.3.

4 Numerical Simulations in Dark Matter Cosmology (Aliki Litsa)

The numerical simulation techniques used in dark matter research are closely related to the physics of the Early Universe, as described by the cosmological model of inflation and by that of structure formation seeded by matter and density perturbations. The following contain a brief account of the large scale structure formation procedure, which can be more thoroughly studied by the reader in Daniel Baumann's notes on Cosmology, or in Scott Dodelson's book on Modern Cosmology [48]. As we have, already, mentioned in section 2.2, inflation is the very mechanism that provides the necessary initial conditions in order for the subsequent structure formation to take place, and lead to the creation of all large scale structures observed today. Such conditions include the scale invariant, adiabatic density perturbations, whose growth is first regulated by the radiation itself, and, at later times, by the Dark Matter component of the Universe. The particular perturbations grow during radiation domination, but their growth slows down as they pass the particle horizon. The result is that a characteristic scale is established, which corresponds to the horizon at the moment of transition to the matter dominated era. Since the gravitational potential is the factor which boosts the growth of such matter perturbations, another way of understanding the effect mentioned above, requires an explanation of the way in which the gravitational potential itself evolves. As we can see in Figure 16 the gravitational potential Φ remains constant while the modes remain outside the horizon. Modes with a wavenumber $k \geq k_{eq}$ (where k_{eq} refers to the characteristic wavenumber at matter-radiation equality) cross the horizon during the radiation domination era. The amplitudes of such modes decrease as a^{-2} , from the time of horizon crossing, until the time of matter-radiation equality, and, therefore, the particular modes enter matter domination significantly decayed. At this point it is important to point out that the perturbation growth proceeds only logarithmically during radiation domination, but it proceeds linearly (and, thus, more intensely) during matter domination. As a result, modes like the ones mentioned above, which enter matter domination with a significantly decayed gravitational potential do not contribute as much to the formation of large structures in the Universe. On the other hand, modes that satisfy $k < k_{eq}$, cross the horizon during the matter era and, therefore, correspond to a gravitational potential which faces minimal decay. These modes, enter the matter dominated era with a significant amplitude and are, therefore, able to contribute to structure formation. At the same time, dark matter fluctuations, below a certain scale, are washed out by random thermal motions. This free-streaming scale corresponds to the comoving distance a particle can travel during the age of the Universe and satisfies $\lambda \propto m_x^{-1}$ [49].

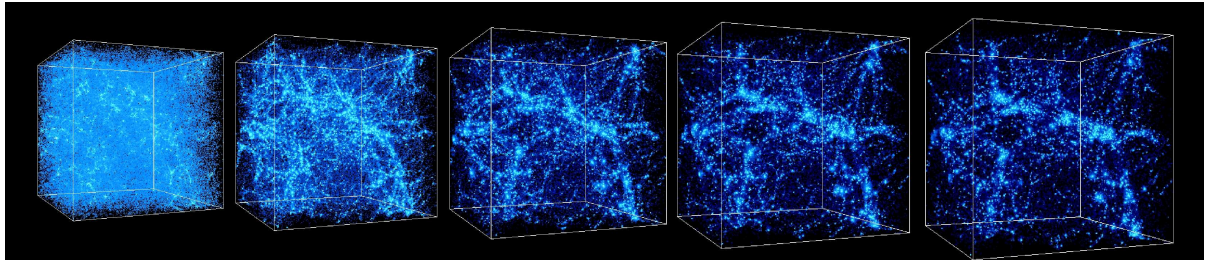


Figure 15: Simulation of formation of the large-scale structure in the Universe (Big Bang, inflation, Cold Dark Matter) <http://cosmicweb.uchicago.edu/> Credits: simulations were performed at the National Center for Supercomputer Applications by Andrey Kravtsov (The University of Chicago) and Anatoly Klypin (New Mexico State University).

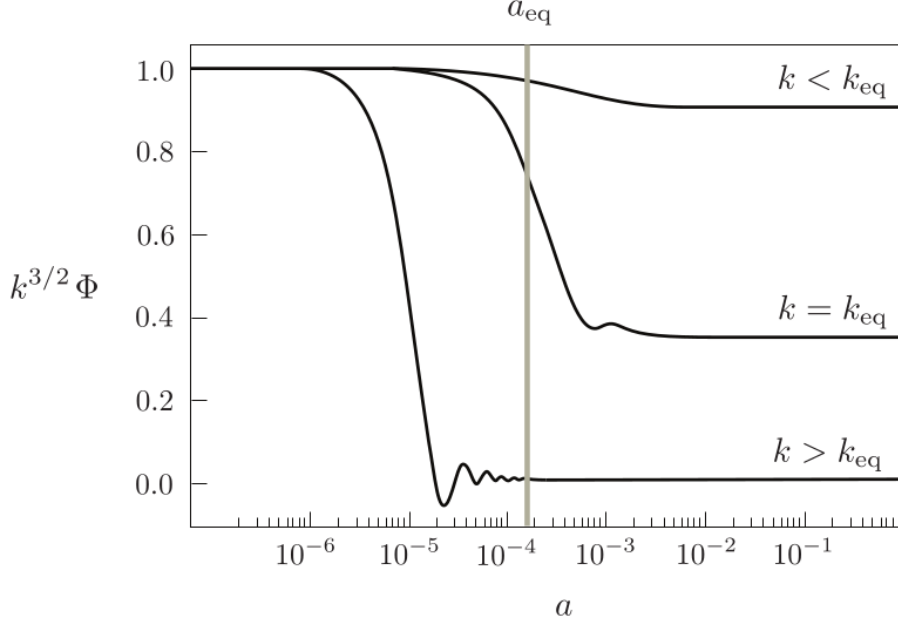


Figure 16: Numerical solutions for the linear evolution of the gravitational potential (taken from Daniel Baumann's notes in Cosmology <https://www.dropbox.com/s/5a6x67n30ssguzv/Chapter4.pdf>)

Having given this short introduction on the processes of perturbation growth and how that affects structure formation, it is time to make the connection with numerical simulation techniques and their importance in dark matter research. Our conclusions from CMB observations, along with the cosmological theory at hand as described above, indicate that very small structures collapse first and, subsequently, merge to form larger structures. We can, therefore, see that a growth from small to larger and larger objects takes place, ultimately leading to the Universe that is observed today. The baryon acoustic oscillation features, as well as all phenomena related to cosmic scales, emerge from linear or slightly non-linear perturbation growth. As, however, structures get smaller and reach cluster and galactic scales, non-linear growth becomes dominant and the analytical approach of the problem is no longer close to reality. The solution to such a problem is provided by the numerical simulation techniques, which allow the evolution of Dark Matter density fluctuations up to the present day, covering a very large range of length scales (from ~ 10 Gpc to ~ 10 pc). The outcome of numerical simulations is not significantly affected by the composition of dark matter (and by any non-gravitational interactions its ingredients may experience), but rather by the initial velocity distributions of such particles during structure formation [50], [51]. Such distributions do not have a very large effect on large scales, they can, however, seriously influence smaller scales that may be washed out if the particles are highly relativistic (as explained in previous paragraph).

The history of numerical simulations in galactic interactions should not necessarily be thought of in terms of computational coding processes, since their first steps took place long before such computational procedures were possible [52]. In 1940, Swedish scientist Erik Holmberg conceived a very creative way of visualizing galaxy interactions, by making use of the fact that both the gravitational and the electric force follow the same inverse square law ($F \propto \frac{1}{r^2}$). Holmberg's experiment included 74 light-bulbs, photocells and galvanometers. After measuring the amount of light received by each cell, he manually moved the light-bulbs towards the cell that received the most light, thus simulating galactic motion in the Universe. Some of the results of the particular experiment are presented in Figure 17. The years following Holmberg's experiment were characterized by the events of World War II, which boosted progress in all scientific, and especially computational, methods due to the increased military research. However, it wasn't until the early 1970s that numerical simulations in cosmology began to truly prosper, thanks to the newly published cosmological theory of inflation in the scientific community [20], [22]. The initial conditions provided by the particular theory, as explained in the first paragraph of the section, along with subsequent imaging results of galaxies provided by the 3D CfA sky survey (more in section 4.1) gave numerical simulation research the necessary tools for attempting to determine the true composition of the mysterious dark matter component [53].

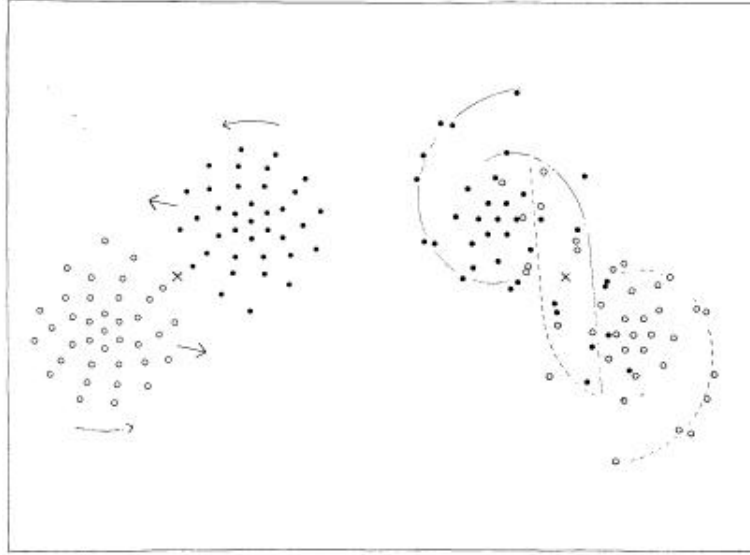


Figure 17: Results of the simulation of a collision between two nebulae. Left panel: two disky galaxies approaching. Right panel: after the collision. From Holmberg (1941) [54].

At this point it is important to briefly discuss the particular numerical simulation methods used in order for the result mentioned above to be achieved. In general, cosmological numerical methods include N-body particle simulations, where the gravitational evolution of the particles is determined by the Poisson-Vlasov equations, in a coordinate system which is comoving with the mean expansion of the Universe. The two main techniques include [55]:

- The *Tree Code* technique, where particles are organized in a hierarchical system, depending on their contribution to the gravitational field. More specifically, particles that are very distant from our spacetime point of interest, and, therefore, have very low contributions to the gravitational potential of the particular point, are related to low order terms in a multipole expansion of the mass distribution. Particles that are closer by correspond to higher order terms of the same expansion.
- The *Particle Mesh* method, where particles are placed on a mesh, in order for a density field to be formed. Adapting the particular mesh according to the needs of the problem leads to the formation of high and low density regions.

Such techniques are used for dark matter research at many different scales, from cosmic scale baryon acoustic oscillation simulations to halo simulations in galactic scales. The results of the particular simulations are compared to results from gravitational lensing and CMB observations, in order for conclusions to be drawn.

4.1 Excluding Hot Dark Matter with Numerical Simulations (Aliki Litsa)

As we have mentioned in section 3.2.1, hot dark matter (HDM) does not constitute a viable candidate for the explanation of the dark matter properties and effects. Despite their limitations and early stage of evolution, numerical methods in the 1980s played the dominant role for the final dismissal of the HDM model (at least in the case of neutrino dominated models).

In the introductory discussion of this section, we mentioned the dependence of the free-streaming scale λ_f on the mass of the candidate particle m_x as $\lambda_f \propto m_x^{-1}$. For the case of HDM, the mass of the neutrino candidate $m_x \sim 30$ eV (according to scientific research carried out in the 1980s) corresponds to a free streaming scale that reaches the size of a large galaxy cluster. Of course, recent measurements of the neutrino mass from neutrino oscillation experiments [56] indicate an even lighter neutrino and, therefore, an even larger λ_x . Since all dark matter fluctuations under the particular scale are damped, the Universe that results from cosmological structure formation, in a HDM model, does not include scales smaller than large galaxy clusters. Therefore, if we assume a HDM cosmological model, the observable Universe today can only be created via top-down procedures, where super-clusters form first, and, then, fragment into galaxies. In the following we are going to examine whether such a Universe can be confirmed by numerical simulation evidence.

The imaging data necessary in order for the numerical simulation efforts to be set in motion were provided in the 1980s, by the 3D CfA redshift survey, which offered information on the positions of a large number of galaxies [53]. During the same decade, various research groups [57, 58, 59, 60] created numerical simulation codes with the purpose of modelling structure growth from the initial conditions of inflation until today. Their goal was to compare their results to data collected by the CfA survey itself, and determine whether the HDM model could be considered a reasonable dark matter model, based on its effects on structure formation on large, as well as small scales. Such numerical simulations of non-linear clustering showed that super-cluster collapse in a HDM Universe must have occurred quite recently at $z_{sc} < 0.5$ [57]. However, limits on galaxy ages acquired from various globular clusters and other stellar populations indicated that galaxy formation has to have taken place before $z \sim 3$. Moreover, since quasars are associated with galaxies, as is suggested by many observations, the abundance of quasars at $z > 2$ was also inconsistent with the top-down neutrino dominated scheme in which superclusters form first: $z_{sc} > z_{gal}$.

Figure 18 presents three HDM models, two CDM models, as well as actual observations made by the CfA survey [61], [53]. We can easily conclude from the plot that HDM simulations provide a rather different Universe density distribution compared to the one we can actually observe. As mentioned in the previous paragraphs, the clustering scale in the case of HDM exceeds the observed scales of galaxy clustering [60], resulting in a much more clustered pattern than the one provided by observations. The particular effect is, also, pronounced in Figure 18 where, in the case of HDM, superclustering is more prominent, while the texture of smaller underlying structures is less visible. The reason behind such an effect lies in the fact that, in the case of HDM, the formation of galaxy superclusters, in regions where collapse has taken place, occurs before everything else, due to the very large characteristic scale that is imprinted at horizon crossing (as explained in the introductory part of section 4).

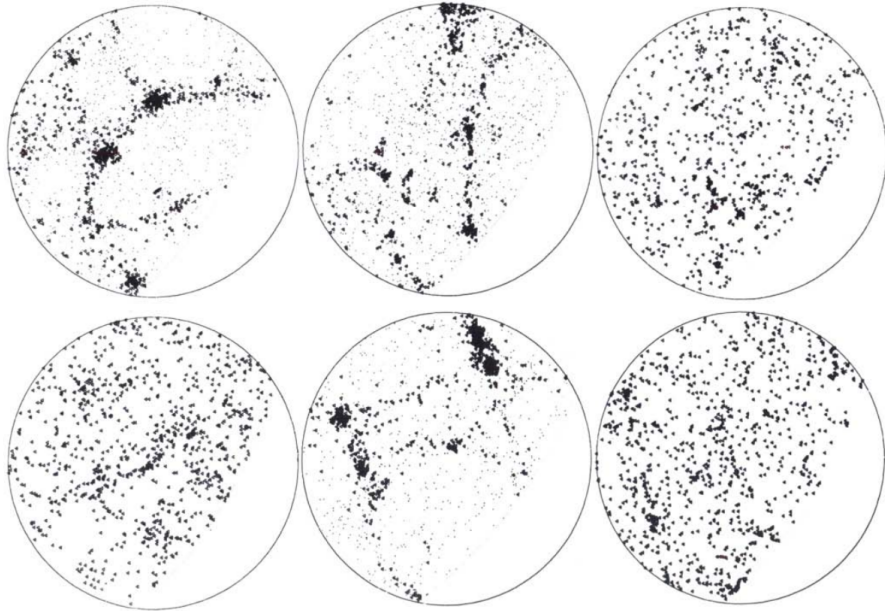


Figure 18: Three HDM models (middle top, middle-bottom and left-top panels), two CDM models (left-bottom and right-bottom panels) and CfA survey results (right-top) [49]

Further numerical simulations performed during the 1980s [62] made use of the (non-linear) *Pancake model* of Galaxy formation [63], which also constitutes a top-down galaxy formation model. The term *pancakes* refers to the thin, dense condensations of gas that are formed from the growth of small inhomogeneities in non-linear gravitational instability theory. After their creation, these condensations, are compressed and heated by shock waves, which leads in their fragmentation into gas clouds. Galaxies and their clusters are formed due to the clumping of these gas clouds. The results of the particular simulations showed that at least 85% of the baryons become so hot, by the associated shock, that they are unable to condense, and, therefore, unable to attract neutrino halos in order to form galaxies. This constituted a serious problem for the HDM argument, since, taking into consideration the primordial nucleosynthesis constraint $\Omega_b \sim 0.1$, baryonic matter does not suffice to produce enough structures which can account for the luminosity observed in the Universe.

Despite any inaccuracies related to the possibly flawed observations of the CfA survey, as well as uncer-

tainties related to galaxy formation, the evidence against the HDM argument were, indeed very convincing from these early stages of dark matter research.

4.2 Physics beyond the CDM model (Marnix Heikamp)

4.2.1 Problems on small scales

We have seen that deviations from the CDM model need to be made to fit the found data. These deviations have implications on the structure and evolution of various cosmological systems and are thus topic of debate amongst astronomers [64]. These discussions focus on the impact that baryons have on the dark matter models that exist, and more generally the interplay between the physics that govern the behaviour of both types of matter. We will first look into the observations, or hints towards physics that extends the CDM model, that have recently been made. For a more informative overview of these problems, the reader is suggested to look at [65] and [64]. We expect the reader to have a basic understanding of galaxies and halos, which could alternatively be obtained by reading section 3.2.1. from [64].

- **Cusp/core problem** If the density of the dark matter halo would be isothermal, it would scale as $\rho(r) \propto r^{-2}$. However, it was found that the density profile is governed by the Navarro-Frenk-White (NFW) power-law [66]:

$$\rho(r) = \frac{\rho_s}{(r/r_s)(1+r/r_s)^2}.$$

Here, r represents the distance to the center and the s subscript denotes a normalization that we shall not investigate. This requires that, in Λ CDM simulations simulations with no other matter than dark matter, the density profiles of the dark matter halo rises steeply at small radii, such that $\rho(r) \propto r^{-\gamma}$, with $\gamma \simeq 0.8 - 1.4$ in this regime [67]. However, observations show that for most low-mass, dark matter dominated galaxies, the density profile flattens to $\gamma \simeq 0 - 0.5$ [65]. Additionally, the amount of dark matter that ought to be in the center is higher than what is observed. These observations imply that the halo is more cored than what is expected from the NFW distribution. The consequence of this effect on the rotation curve problem is shown in figure 19. Here, we see that the rotation curve rises quicker for the NFW power-law than for the observations.

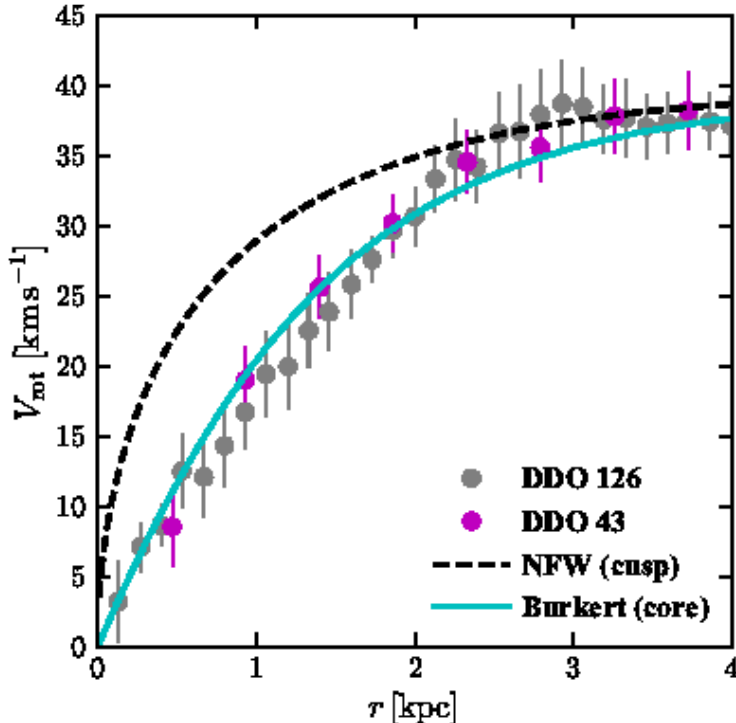


Figure 19: Rotational velocity distribution for varius radii according to the NFW model and the fitted data to a flatter density distribution. Figure taken from [65].

- Missing satellites problem

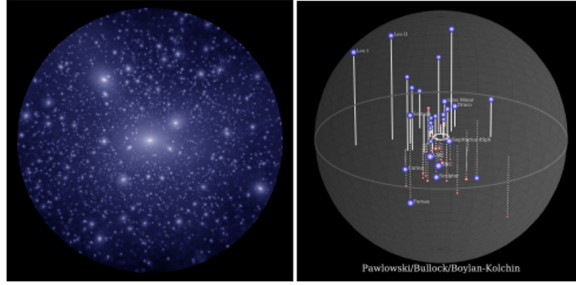


Figure 20: Missing satellite problem. Figure taken from [65].

The former problem arises from the smooth distribution of matter within a halo, whereas the missing satellites problem comes from the non-smooth distribution parts. Halos form by accretion of smaller halos [64]. However, this accretion process is not complete, causing a substructure that is not smooth. When numerical simulations achieved higher resolution to distinguish the different components of a halo, it was found that Milky Way-like galaxies have as many substructures as galaxy clusters have. Even though higher resolution surveys may find more faint dwarf galaxies, the Milky Way does not appear to have enough satellite galaxies to be in accordance with numerical predictions [65].

- **Too big to fail** A direct follow-up of the previous problem is the too big to fail (TBTF) problem. It was found that the discovery that the circular velocities of the largest subhalos in the CDM dark matter-only simulations were too high to be in accordance with the large Milky Way classical dwarfs [64]. This means that these subhalos, which ought to be big and massive enough to make stars and thus be visible, are not found in measurements.
- **Tully-Fisher relation** The Tully-Fisher relation is one of the oldest distance measurements that exists for the Milky Way [68]. It relates the luminosity of a galaxy with the depth of the potential well [64]. However, this relation appears to break down when considering the halo mass and the baryonic mass of a galaxy. It seems that the dwarf galaxies live in smaller halos than expected [64]. Thus, when CDM is the correct way of describing dark matter, there must exist a TBTF problem for small galaxies [64].

4.2.2 Mass of galaxies and dark matter halos

We have just been exposed to four problems that are frequently recurring in literature on problems with CDM. Though it could be the case that these problems are not connected, we aim to find a common interpretation that may explain multiple, or all, stated problems. We find such a solution in the mapping between the masses of the dark matter haloes and the associated galaxies. This relation is especially uncertain on small scales [64].

The last three problems arise as a consequence of the mapping between the observed behaviour, specifically the kinematics, of baryons and the halo mass. We find a discrepancy between the halo that is simulated from CDM and the observed abundance of galaxies. So, in essence, the problem at hand reduces to a counting problem. The former conclusion holds when the current mapping is correct. When this is not the case¹, the main problem reduces to the cusp/core problem. We know that the ratio for the virial velocity to the velocity of the baryonic tracer is higher in cored halos, so when we know which halos inhabit which galaxies, we would be able to confidently interpret galaxy abundances. I.e., we would know whether we would actually have a counting problem or a cusp/core problem.

It is worth mentioning that when we would be more confident about how to compare galaxies with halos, we would be able to get to the root of the cusp/core problem [64]. The amount of energy that is required to move dark matter towards the edges of a galaxy depends on the characteristics of the potential well, and thus on the halo mass. So, when we would know more about the relation between the galaxies to the halos, we would be able to (dis)prove a CDM + baryon physics interpretation, that can explain the dark matter densities as a function of the galaxy mass. This gives rise to a sense of urgency to find limits on the halo mass.

¹This could for instance occur due to systematic issues or due to a more fundamental error in the CDM simulations, giving rise to the dark matter mass-profile.

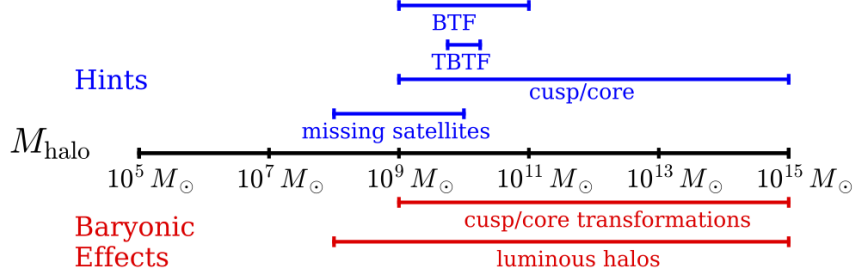


Figure 21: Above: An overview of the various halo masses where hints towards deviations from Λ CDM have been found. Below: An expectation of the range in which baryons are expected to have influence on the structure and evolution of galactic halos [64].

In the top part of figure 21, the different hints are plotted towards CDM being an inaccurate description of dark matter at mass scales in the range 10^9 – $10^{15} M_{\odot}$. In the bottom part, the scales at which baryonic effects provide solutions is given.

4.2.3 Considering baryonic matter

The four issues that were put forth in the previous subsection have sparked immense interest from both particle and astrophysicists. Together, the people in these fields have come up with many dark matter models that attempt to adapt dark matter halos with $M_{\text{vir}} \sim 10^{8\text{--}15} M_{\odot}$ (Here, the subscript denotes some typical scale related to the virial radius, see for instance [69]). These models mainly consist of predictions that disregard the impact of baryons, for reasons explained in section 3.1. We have readily seen that baryons have a minor contribution to the energy budget of the system, but they do have an important contribution to the dynamics of a system. Thus, we should consider baryons when extending the CDM model to explain the aforementioned problems that arise. We shall thus hint towards how considering baryons alleviates all of the mentioned problems.

- **Cusp/core problem** Baryons appeared, from early hydrodynamic simulations, to cool down in halos, and deepened the gravitational well, pulling in dark matter towards the center of a galaxy. More on hydrodynamical simulations in section 4.3.1. Thus, intensifying the cusp/core problem [64]. Increasing the spatial resolution aided in solving these problems [70]. Unfortunately, simulations have not yet been able to explain the unexpected density profile at low radii. Some simulations create denser cores, whereas others find low density cusps. This signifies that it is yet uncertain how baryonic matter interacts with the dark matter halo and even if baryonic matter is the sole source of this odd finding [64]. Baryons can affect the central density at halo mass scales of order $10^{9\text{--}15} M_{\odot}$ [64, 65]. Thus, studies are continuously performed to uncover the physics that hides in these regimes.
- **Missing satellites problem** The solution towards this problem comes from combining three physical effects [64]. Firstly, we should consider the subhalo mass function. After all, adding baryons to the system allows for a lower dark matter abundance in various ways. Secondly, the mapping of the observed properties to those that arise from simulations. The interested reader is directed to [64] or [65] to find out more about the implications this has. The third component, and of most relevance, comes from the probability that visible baryons may exist in subhalos. This is of most importance in dwarf galaxies. These reasons combined give convincing arguments towards baryonic matter, partially, solving the missing satellite problem. Thus, the new area where research should go into is around and below $\sim 10^8 M_{\odot}$. In that regime, galaxy exist without baryons [64].
- **Too big to fail** We already saw that using hydrodynamic simulations of CDM can solve some of the faced issues by introducing baryons. The same type of simulation can fix this problem. Baryons can push dark matter out of the center of the halos, causing the central density to drop and thus partially resolving this issue. This works on scales around $10^{10} M_{\odot}$ and does not solve all issues [64]. Especially, Fornax is an interesting case to consider for the interested reader [71].
- **Tully-Fisher relation** The most convincing hint towards solving this obstacle is by looking into the highest velocity material in galaxies is located in gas with too low column densities to be measured. This causes the velocity measurements to be inaccurate. It is thus appealing to consider the interpretation of the rotation curve as the problem and not the efficiency of star formation [64].

4.2.4 Numerical simulation

We have seen that adding baryonic matter aids in some of the presented problems. However, the interaction between baryonic and dark matter is still topic of heated debate. While galaxies form, the present gas cools and falls inwards. This increases the central density and is referred to as 'adiabatic contraction'. This halo contraction appears in most hydrodynamical simulations, but does not succeed in reproducing the observed rotation curves [72, 73]. To fit the numerical result to the observed data, we need a halo that does not contract [72, 74] and potentially even expands [75]. Thus, we need to specify a process that can, at least, counteract this contraction. For instance, the kinematics of the bulk gas can cause considerable fluctuations in the gravitational potential of a galaxy [76, 77]. This leads to a reduced energy density at the inner regions of a galaxy. Indeed, a simulation that attempted to simulate a dwarf galaxy with a cored dark matter profile at $z = 0$ by applying CDM, having several characteristics of dwarf galaxies [70]. The flattening that was observed in the analysis turned out to be a consequence of small starbursts, located near the center of a young galaxy and creating pockets of fastly expanding gas, which transfer energy from baryonic to dark matter [78].

One of the more noteworthy findings on this topic comes from including baryon physics such that CDM and non-CDM predictions grow closer together, see for instance [65] for the relevance of this. We have seen that the influence of baryons becomes considerable for scales $10^{8-15} M_{\odot}$, so they affect the halos in figure 21. Thus, although we cannot say that baryons explain all small-scale problems that arise from CDM, we can say that it aids in finding an all-round theory.

4.3 Effect of baryons on Numerical Simulations (Stan Bovenschen)

Previously in this section, we have seen several implications where numerical simulations are needed in our search for dark matter. Dark matter simulations usually are simplified by doing simulations with the dark matter component only. Once we know how this single component Universe works, other components can be added. Now, to make a simulation of only dark matter is relatively easy because dark matter does not, or barely, interact with itself nor with baryons. Therefore, not taking in account interactions is a pretty good estimate, yet not entirely correct since the dark matter distribution is coupled to the baryonic distribution in the Universe. Once adding the baryonic component we need to take into account not only the interactions baryons have with each other but also with dark matter. We know that baryons interact strongly in different ways, due to baryons galaxies can form and so can all other known structures. We need to know exactly how baryons behave throughout the Universe in order to be able to make a model with the baryonic component. This model will tell us more about the distributions of dark matter since the components are gravitationally bound. However, modeling all the baryonic matter of the Universe brings some complications with it. Section 4.2.1 gives a description of some of those difficulties. Following in this section we will discuss some effects that baryonic matter has on galaxies and on dark matter.

4.3.1 Baryonic matter in hydrodynamics

Baryonic matter can be treated like a fluid when the mean free path of a particle is much smaller than the length scale of the fluid: $\lambda_{\text{mfp}} \ll L$. Also collisions have to happen frequent enough for the fluid to have a distribution close to Maxwellian. This is the case for baryonic gas in most parts of the Universe [79]. Since we can neglect viscosity but not the magnetic field of the interstellar medium we have to deal with an ideal magneto-hydrodynamic fluid. This way we can explain several characteristics of baryonic matter in galaxies. The granulation in spiral arms in galaxies for example arise by the Parker instability, which states that a uniform distribution of the ISM is unstable. Imagine a patch of gas with frozen-in magnetic field lines where gravity exerts a force in the downward direction. We insert a perturbation (see figure 22) in which the magnetic field lines are bend. The gas will flow down along the field lines to the side, as a consequence the middle, perturbed, part will have a lower density and become buoyant. The perturbation grows larger and the gas separates to both sides of the perturbation finally the perturbation stops by the tension of the magnetic field lines. A gap within a spiral arm arises [79]. Figure 23 shows a modeled image of galaxy M33 where one can see the granulated spiral arms.

Since most of the matter in the Universe is in the form of gas in the interstellar medium (ISM), we do not necessarily have to look directly to the mass distribution of more compact objects like stars. Indirectly, however, stars and other baryonic objects are influencing the ISM constantly. Supernovae, for example, inject an enormous amount of matter in the ISM, which is called feedback (also mentioned in section 4.3.3). The evolution of the ISM throughout the age of the Universe has to do with many parameters, this is hard to model. Therefore techniques are developed to make calculations easier. The smoothed particle hydrodynamics (SPH) approach is an example of such a technique, which will be discussed in the next section.

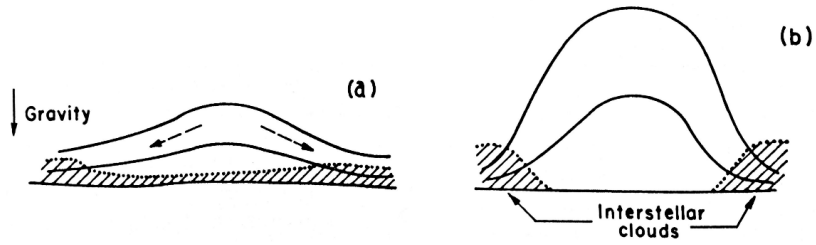


Figure 22: Illustration of the Parker instability. (a) shows a small initial perturbation. (b) shows the result where the interstellar could is separated into two peaces [79].

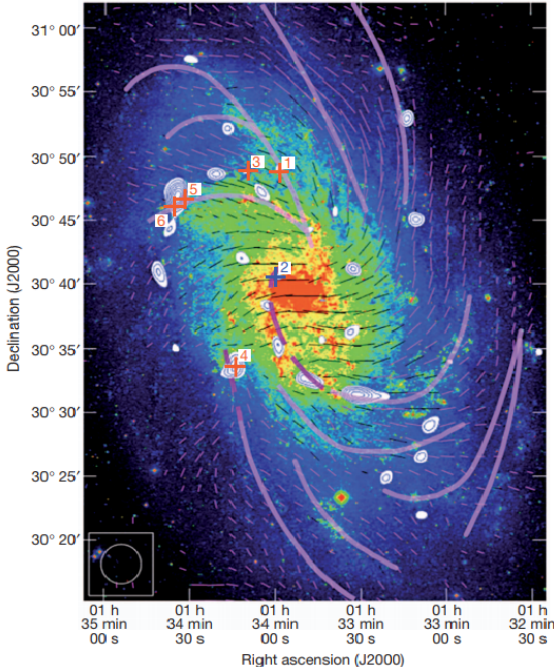


Figure 23: Optical image of galaxy M33. The color decomposition shows different levels of peak intensity of the Gaussian distribution [80]. The fat purple lines are aligned with the spiral arms one can see the irregular shape of baryonic matter as a result of the Parker instability.

4.3.2 Numerical techniques

One can distinguish two different reference frames for modeling a fluid-dynamical problem. We have the Eulerian approach, which has its reference frame at a fixed point in space and the Lagrangian approach, which has a reference frame that is co-moving with a fluid element . This difference can also be explained by looking at the derivatives that are used for the fluid dynamical variables in both frames. The relation between the derivatives of both frames is [79]:

$$\frac{dQ}{dt} = \frac{\partial Q}{\partial t} + \mathbf{v} \cdot \nabla Q,$$

where $\frac{dQ}{dt}$ is the Lagrangian derivative and $\frac{\partial Q}{\partial t}$ the Eulerian derivative. While doing fluid dynamics we do not necessarily have to use a grid to model astrophysical properties. Instead the SPH technique can be used. This technique uses the Lagrangian, co-moving, approach to calculate the wanted parameters. In addition, it is a particle method which makes use of analytical differentiation of interpolation formulae [81]. In other words, the particles are discretized and obey the implemented interactions between each other, just like a

fluid. Mathematically we can see the discretization of particles as follows, starting out with a scalar function $f(\mathbf{r})$:

$$f(\mathbf{r}) = \int_V f(\mathbf{r}') \delta(\mathbf{r}-\mathbf{r}') d\mathbf{r}'$$

where \mathbf{r} ranges over a volume V . Once we generalize the Dirac delta function, still keeping it normalized, and expand the resulting expression we end up with the following discretized expression [81]:

$$f(\mathbf{r}) \approx \sum_i \frac{m_i}{\rho_i} f(\mathbf{r}_i) W(\mathbf{r}-\mathbf{r}_i, h).$$

Here, $W(\mathbf{r}-\mathbf{r}_i, h)$ is the generalization of δ , the particles has been given a mass of $m = \rho(\mathbf{r}') d\mathbf{r}$ and i goes from 1 to N , where N is the number of particles. This discretization of $f(\mathbf{r})$ results in the energy and momentum equations becoming ordinary differential equations [82], which we can understand and interpret. Modeling a hydrodynamics problem using SPH has certain advantages, namely [55]: this technique is automatically adaptive and has a higher resolution in collapsing regions. The latter is important for the formation of stars, which plays a big role in the history of baryons. SPH also has some disadvantages like the fact that lower density regions are modeled with less precision. Also, an artificial viscosity has to be added to compensate for the lack of entropy when shocks occur. This extra viscosity makes the method more dissipative [55]. In order to get rid of those disadvantages people are looking for improvements of the SPH technique.

Another well known technique for modeling baryonic matter is Adaptive Mesh Refinement (AMR). This technique is based on the Eulerian frame, where the fluid flow is discretized in space. Here the grid where the Euler equations are calculated on is adapted to be finer on the places where a higher accuracy is needed. This method has as advantages that it describes shocks very well and it has little noise. Also, instabilities, like the Parker instability, are well modeled. However the AMR algorithm is more complex and it therefore takes longer to run [55].

It is clear that both of those methods have some flaws. The obvious solution for the problems in both techniques is combining the two. This results in an adaptive moving grid [83]. With this combined technique we can start to think about modeling galaxies.

4.3.3 Modeling galaxies

In several early simulations of the galaxy distribution, all the galaxies were approximated to behave the same way. This is, of course, not true since there are so many micro- and macroscopic effects that we have to account for. It is possible to precisely model galaxies by using the previously described techniques and our knowledge of magneto-hydrodynamics. When 'creating' a galaxy one has to take into account that a galaxy is not adiabatic, galaxies are for example cooling due to radiation emission. For this non-adiabatic processes cooling functions can be implemented to calculate what will happen to, for example, the cooling rate as function of density and the temperature [84].

Due to the non-adiabaticity of the galaxy, certain regions will cool. The gas pressure will decrease and star formation can happen by fragmentation [84]. The adaptable grid will make sure that we will capture every effect that plays a role on these smaller scales. For star formation to happen, a gas could will need to meet the Jeans limit, where a cloud of a certain density is smaller than its Jeans length. Once this is the case we can estimate the formation time by the free fall timescale. By implementing the Schmidt law we can estimate how often star formation will happen [85]. Star formation is, however, not one-hundred percent efficient. It turns out that the star formation rate (SFR) per free fall time is only: $SRF/\tau_{ff} \approx 0.01$ [86]. In galaxies we also have to deal with dying stars, which can be really messy. Especially supernovae and jets from neutron stars are ejecting huge amounts of material in the interstellar medium. As mentioned, these processes are called Feedback processes. Feedback happens on small scales, yet it can have a great effect on larger, galactic scale [87]. Figure 24 is an example of a modeled galaxy where all the previously discussed properties are processed.

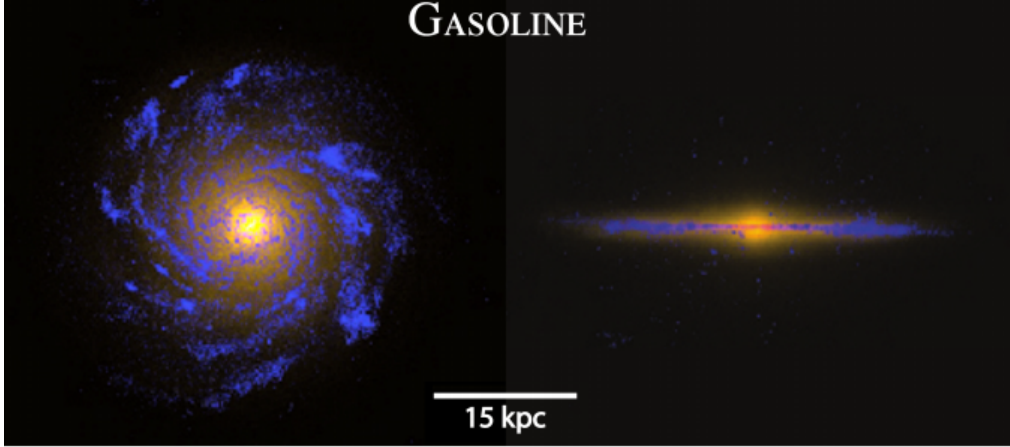


Figure 24: Optical and UV composite images of the Eris galaxy, a Milky Way like galaxy. [87]

4.3.4 Stellar streams

A stellar stream is a band of many stars that are aligned within the galaxy. Every star in the stream follows the same track around the galaxy. These stars are supposedly all drifting away from the same cluster where they formed. The stellar streams have more or less a constant stellar density along its length. The existence of star streams was determined in 1996 [88]. Later, in 2001, it became clear that the streams form from tidal deformation in clusters [89].

Both the cold and warm dark matter models (as explained in section 3.2.2 and 3.2.3) predict that smaller structures than dwarf galaxies (i.e. $M < 10^7 M_\odot$) will be completely dark matter dominated, these dark matter halos are obviously hard to locate since they do not emit radiation. A possible way of detecting them could be by looking at the stellar streams. Once coming close enough, the small scale dark matter halos would be able to gravitationally interact with the stars in the stream by pushing them out of the stream. This way a gap appears in the stream which we will be able to detect [90].

However, we have to be careful with our conclusions since a gap in such a stellar stream could also be an effect of baryonic matter. In figure 25 the stellar stream Pal 5 that has been modeled and displayed. The figure shows a clear gap at $-0.4^\circ < \phi < 0.2^\circ$, which is exactly what we are looking for when trying to detect dark matter subhalos. Unfortunately, this gap has been made by the Milky Way bar and not by a dark matter halo [91]. It is therefore of great importance that we can distinguish baryonic effects from dark matter effects.

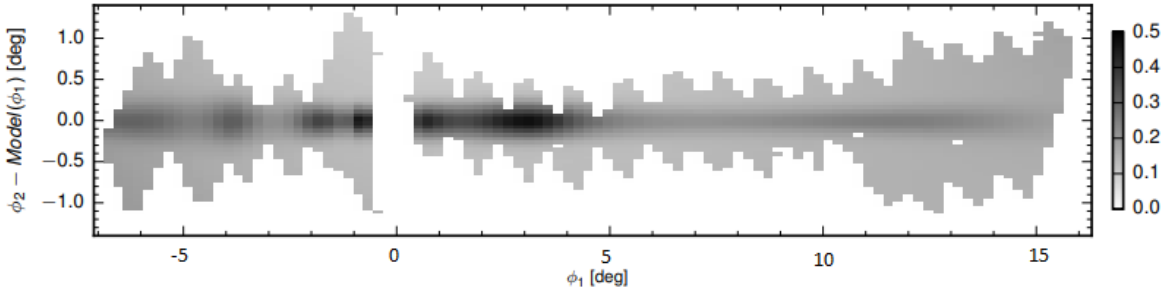


Figure 25: Density distribution of stars in the Pal 5 stellar stream, predicted by the maximum likelihood model. With a gap at $-0.4^\circ < \phi < 0.2^\circ$ which is swept away by the Milky Way bar [91].

4.3.5 Future considerations (Marnix Heikamp)

Slowly, though steadily, more and more studies are investigating this contribution of baryons to the theory of dark matter. Two astronomical systems are frequently used: isolated dwarf galaxies and Milky Way like galaxies. The former is chosen as the computational costs for a high spatial resolution result is relatively

low compared to more massive systems. Considering that hydrodynamic simulations are, when important processes such as radiative transfer are ignored, at least an order of magnitude more complicated to execute than dark matter-only simulations [64]. This makes the choice for isolated dwarf galaxies apparent. Studying Milky Way like galaxies is relevant due to the missing satellites and TBTF problems [64]. Additionally, studying stellar streams will provide more insights in the nature of dark matter.

4.4 Particle physics solutions (Marnix Heikamp)

This far, we have considered the combination of dark energy with cold dark matter as the most prevalent theory to describe the Universe. However, we saw that there are cracks appearing on small scales. We also saw that adding baryons to our numerical simulations may alleviate some of these issues. Unfortunately, there still exist discrepancies between observations and theoretical predictions. Thus, it may prove worthy to look beyond non-relativistic and collisionless dark matter as described by CDM.

4.4.1 Self-interacting dark matter (SIDM)

We should consider the possibility of interaction which is most basically described by two particles interacting with an isotropic, velocity independent, elastic scattering cross-section [92, 93]. A reasonable mean free path of such a particle would be between 1 kpc and 1 Mpc when $\rho_\chi \sim 0.4 \text{ GeV/cm}^3$ (which occurs at radii similar to the distance from the center of the Milky Way to the Sun) [92]. Dependent on the precise interaction and mean free path, the mass of these particles is in the range 1 MeV and 10 GeV [92]. It must be noted that for some time, this type of interaction was considered highly unlikely as a result of three observations [93]: the shape of the halo, halo evaporation and cores in galaxy clusters. From the latter two of these observations, it was found that the cross section had to be constrained by, respectively, $\sigma/m \lesssim 0.3 \text{ cm}^2\text{g}^{-1}$ and $\sigma/m \lesssim 0.1 \text{ cm}^2\text{g}^{-1}$. These constraints are already stringent but considering the halo shape gives a more stringent restraint: $\sigma/m \lesssim 0.02 \text{ cm}^2\text{g}^{-1}$ [93]. Such a low cross section indicates that this velocity independent scattering cannot explain the cores in small galaxies and low surface brightness galaxies [93]. As SIDM was thought of to explain such characteristics, this is particularly unfortunate.

Luckily, the stringency of these upperlimits has recently become subject of debate [93]. The studies that set these limits had incorrectly accounted for the mass contribution from outside the core towards the ellipticity of the projected gravitational potential. The real values are thus likely higher than the previously given constraints [94]. We then find that the overlap between CDM and SIDM is substantial for $\sigma/m \sim 1 \text{ cm}^2\text{g}^{-1}$ [94]. Additionally, it was found that the influence of the central density in a dark matter halo limits the cross section more than the shape of the halos [93, 94].

4.4.2 Fuzzy dark matter (FDM)

Another solution to the small scale problems may come from FDM. The De Broglie wavelength of such a particle would become relevant at astrophysical scales. The lightness (the expected mass was set to $m \sim 10^{-22} \text{ eV}$ [95]) and the quantum behaviour of such particles leads to intriguing pathways to solve the aforementioned problems using the Heisenberg uncertainty principle [96]. Such high wavelengths can suppress cusping behaviour and reduce the amount of low mass halos [95]. An important source of constraining the characteristics of such particles comes from the Lyman- α forest. This was used to set a lower limit on the particle mass, $m > 20 \cdot 10^{-22} \text{ eV}$ [97].

4.4.3 Warm dark matter (WDM)

Particles with thermal velocities at early times have been considered to explain the kind of particles that make up dark matter. Such particles would behave as WDM [98]. Several ideas have been suggested with regards to which particles WDM is comprised of, but the most studied example is the sterile neutrino. Having such a particle is described by the neutrino minimal standard model ν MSM [99]. These particles are relativistic when they decouple from the primordial plasma. That allows these particles to flow out of small perturbations, eventually explaining a cutoff in the matter density spectrum, and suppressing structure formation at small scales [98]. Numerical simulations show that there is no observable difference at scales $\gtrsim 1 \text{ Mpc}$ as the structure formation occurs in comparable ways. Additionally, the CMB radiation is also found with WDM [100].

Returning to the too big to fail problem, less vigorous assumptions have to be made when explaining this problem with WDM than with SIDM [101]. Now, structure formation will occur later than in CDM models [98]. A useful attribute of this problem is that it will set a limit on the particle mass, as that governs the amount of halos that will be produced, which can be compared to observations. A lower limit for WDM

particles is found by performing numerical simulations on the formation of halos and was found to be 1.5 or 1.6 keV, dependent on the amount of observed satellites that are used as comparison [98].

Unfortunately, a contradiction arises when considering dwarf galaxies ($M \sim 10^{10} M_{\odot}$) [102]. Simulations were performed to create halos, of which the size of the core was in good agreement with the theoretical predictions. When considering cores that are of reasonable size ($r \sim 1$ kpc), particles, with mass ~ 0.1 keV, are required to produce such cores. However, such particles could never form dwarf galaxies due to a necessary higher particle mass [98, 102]. Thus, warm dark matter particles cannot explain cored density profiles in dwarf galaxies.

5 Modified Newtonian Dynamics (Marnix Heikamp)

So far, we have explained the characteristics of dark matter. However, we have not yet considered the possibility of an alternative theory for gravity. After all, the problem that arises from flat rotation curves can be solved by applying at least one of two different solution concepts:

1. There exists invisible matter
2. Newton's laws do not hold for galaxies [103].

Concept 1 points to dark matter, concept 2 to a different theory of gravity. An example of such a theory is the modified Newtonian dynamics (MOND). It turns out that such a theory can explain the unexpected shape of the rotation curve. In this section, we will describe the theory, and consecutively elaborate on the complications that MOND faces; arising from the CMB, gravitational waves and the bullet cluster.

5.1 Milgrom's law

Although Newton's laws have been widely tested in high-acceleration environments, they haven't been tested in the realm where objects undergo low acceleration, which happens at the outer edges of galaxies [104]. Thus, we can introduce a constant a_0 , with units of acceleration, and state that Newtonian physics applies when $a_0 \gg a$. Then, this paves the way towards a modified expression of the Newtonian force:

$$F_N = m\mu\left(\frac{a}{a_0}\right)a, \quad (1)$$

where m is the gravitational mass of the object, a is the acceleration, and the interpolation function is:

$$\mu(x) \rightarrow \begin{cases} 1 & \text{for } x \gg 1 \\ x & \text{for } x \ll 1 \end{cases} \quad (2)$$

So, in the regime where Newtonian physics breaks down according to MOND, $a \ll a_0$, we find that:

$$F_N = m\frac{a^2}{a_0}.$$

Now, for objects with mass m in a circular orbit (which we approximate the stars in our galaxy to follow), we have that:

$$\begin{aligned} \frac{GMm}{r^2} &= m\frac{(v^2/r)^2}{a_0} \\ v^4 &= \frac{GMma_0r^2}{mr^2} \\ &= GMa_0 \end{aligned}$$

Here, a_0 is experimentally found to be $\sim 10^{-8} \text{ ms}^{-2}$ [103, 104]. This indeed gives rise to a rotation velocity that is independent of r , such that the rotation velocity is flat, implying there is no need for dark matter.

5.2 Conservation of momentum

We can, thus, see that Milgrom's law, as written in equation 1, solves the rotation curve problem. However, this is merely a law, which should be derived from a universal force law and, furthermore, does not uphold the principle of conservation of momentum. Let us consider a system in which two masses, m_1 and m_2 are small enough to be in the weak acceleration limit, and in rest on the x-axis. Now, we can express the change in momentum of the system as follows:

$$\begin{aligned} \dot{p} &= \dot{p}_1 + \dot{p}_2 = m_1\dot{v}_1 - m_2\dot{v}_2 = ma_1 - ma_2 \\ &= m_1\sqrt{\frac{F_Na_0}{m_1}} - m_2\sqrt{\frac{F_Na_0}{m_2}} = \sqrt{F_Na_0}(\sqrt{m_1} - \sqrt{m_2}). \end{aligned}$$

We can immediately see that this does not equal 0 when $m_1 \neq m_2$, thus violating the principle of the conservation of momentum. Thus, equation 1 cannot be more than an approximation of a more heuristic

force law. Such a law would have to be derived from a variational and action principle, leading to a, classical, MOND theory.

To change the dynamics such that they will give Milgrom's law, the classical action provides a good starting point. We describe a system in which a set of particles move in a gravitational field that arises from the matter density, $\rho = \sum_i m_i \delta(x - x_i)$ and is linked to a potential, Φ_N , such that:

$$S_N = S_{\text{kin}} + S_{\text{in}} + S_{\text{grav}} = \int \frac{\rho v}{2} d^3x dt - \int \rho \Phi d^3x dt - \int \frac{|\nabla \Phi_N|^2}{8\pi G} d^3x dt$$

Now, we know that $d^2x/dt^2 = -\nabla \Phi_N$, which can be used to find $\nabla^2 \Phi_N = 4\pi G \rho$. We can now modify the gravitational action. When we do this, the equation of motion remains in tact, but we will find a different Poisson equation [103]. For the gravitational action, we derive:

$$S_{\text{grav, BM}} = - \int \frac{a_0^2 F(|\nabla \Phi|^2 a_0^2)}{8\pi G} d^3x dt,$$

where F represents any dimensionless function. We can vary this with respect to Φ , to find:

$$\nabla \left[\mu \left(\frac{|\nabla \Phi|}{a_0} \right) \nabla \Phi \right] = 4\pi G \rho,$$

where $\mu(x) = F(\sqrt{x})$ and $\mu(x)$ still satisfies equation 2. Thus, when $|\nabla \Phi| \ll a_0$, we find that the potential becomes non-linear, which is contradictory to general relativity, which predicts linear equations in the weak-field limit [105]. This means that we can constrain MOND by considering general relativity and gravitational waves (GWs) in particular.

Besides this issue, several other fundamental problems have arisen of which most have been solved. For instance, the notion that this theory was not generally covariant, which has been solved by Bekenstein by extending the theory to a more general one [106]. One issue has not been solved yet and it is the main reason why MOND is usually considered to be incorrect, which arises from considering the shape of the angular power spectrum of the CMB.

5.3 MOND and the CMB

MOND works well on small scales, but when trying to apply it to explain the CMB, it fails [107]. An extended² version of MOND theory that only includes baryons cannot explain the anisotropies in the CMB, due to the damping of perturbations during recombination [107, 108]. The peaks in the power spectrum cannot all be explained. In certain models, the first two peaks are compatible within MOND, but the third peak cannot be matched, unlike for CDM models as can be seen in figure 26 [108]. As long as this issue has not been resolved, we cannot deem MOND a valid theory.

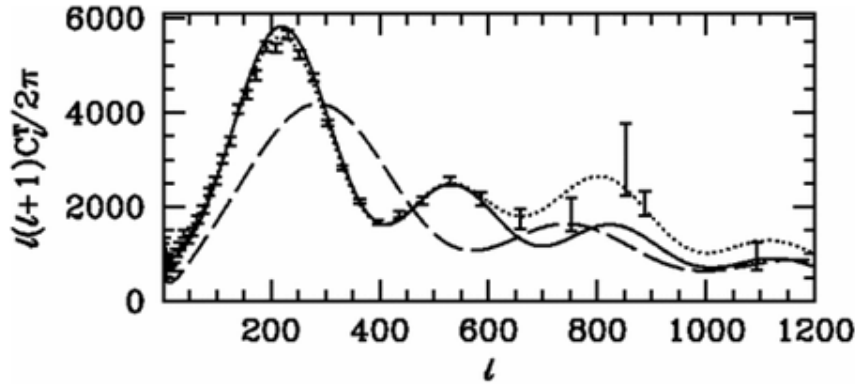


Figure 26: The angular powerspectrum of the CMB for a MOND Universe with $\Omega_\Lambda = 0.78$, $\Omega_\nu = 0.17$ and $\Omega_B = 0.05$ (solid line), $\Omega_\Lambda = 0.95$ and $\Omega_B = 0.05$ (dashed line) and the Λ CDM model (dotted line). A collection of datapoints on the CMB with corresponding errorbars is overplotted. Figure adapted from [107].

²Extended by considering relativistic extensions, by for instance the TeVeS model [106]

5.4 Gravitational waves

Additionally, problems arise for gravitational wave detections. There are two ways in which MOND can alter gravitational wave physics [105]. Firstly, MOND can violate the equivalence principle as it is an acceleration based theory. This would imply that GWs can propagate with a speed that is less than the speed of light. Secondly, we just saw that the Poisson equation is non-linear in the weak-field limit, so GWs could be explained by non-linear equations.

Let's first delve into the first claim. When GWs propagate with $c_g < 1$, where the speed of light, $c = 1$, we must conclude that the arrival times of an electromagnetic signal and the gravitational wave that originate from the same source cannot be the same. However, a recent detection of a GW coming from an inspiraling neutron star binary, of which an electromagnetic counterpart was measured, was made and the time between the arrivals turned out to be 1.7 seconds [109, 110]. This implies that the speed of gravitational waves is equal to the speed of light as that time difference can be explained by the Shapiro time [111]. Additionally, when $c_g < 1$, highly energetic cosmic rays that travel with $v \rightarrow 1$ will lose energy via Cherenkov radiation with a rate dependent on $1 - c_g$. Observing such cosmic rays on Earth allows for a lower bound on c_g causing the rate dependence to be $1 - c_g \lesssim 10^{-15}$ [112, 113]. Thus, it is very unlikely that the speed of gravitational waves is less than the speed of light. In MONDian theories, the speed of gravitational waves depends on the gravitational potential and cannot generically be set to 1, thus making these theories inaccurate.

Regarding the second claim on the non-linearity of the gravitational wave dynamics, we can deduce the following. When these dynamics would indeed be non-linear, the GWs that originate from black hole mergers could interact with themselves. However, LIGO's observation of a black hole merger in 2014 showed no such interaction as the observed signal was consistent with predictions made by general relativity [114]. Therefore, we don't require such a scrambling effect, so we would expect that gravitational waves should satisfy linear equations of motions in the weak-field limit.

We can thus conclude that MOND theories must be heavily constrained by the principles arising from gravitational waves. This implies that it becomes questionable whether MOND is an applicable theory, let alone explain the problems that the theory of dark matter attempts to explain.

5.5 Bullet cluster

The bullet cluster (more formally known as 1E0657-56) merger is a cluster that has given many insights, which we have hinted towards before. Here, we will consider the implications that it has on MOND. At the simplest level, this system seems to disprove MOND [115]. In MOND, gravity is expected to traverse the trace of light and would thus not be able to explain the lensing characteristics of the bullet cluster [116]. This happens because the gravitational center is not aligned with the photometric center, indicating that spacetime might be anisotropic [117]. However, bullet clusters also turn out to be difficult for Λ CDM, as the collision velocity (~ 4700 kms $^{-1}$) is extremely unlikely in this theory [118]. A way around this problem for MOND has been proposed by [119] and has been verified by [117]. Here, a metric is conceived that is comparable to the Schwarzschild metric, with one change. The spatial distance r is replaced by a distance, $R = r(f(v(r)))$. Under certain assumptions, this simplifies to MOND as proposed by Milgrom. This form of MOND can explain the characteristics of the bullet cluster and fits the rotation curve data as well. This may thus explain the missing matter problem [120].

We thus need a special form of MOND to explain the problems that are more generally explained by the theory of dark matter. When also considering the consequences of the recent GWs detection, it becomes tricky to use the theory of MOND as these detections give strong constraints on the possible MOND theories. Then, including the CMB anisotropies makes MOND an unlikely theory.

References

- [1] Jan H Oort. The force exerted by the stellar system in the direction perpendicular to the galactic plane and some related problems. *Bulletin of the Astronomical Institutes of the Netherlands*, 6:249, 1932.
- [2] F. Zwicky. Die Rotverschiebung von extragalaktischen Nebeln. *Helv. Phys. Acta*, 6:110–127, 1933. [Gen. Rel. Grav.41,207(2009)].
- [3] Vera C. Rubin and W. Kent Ford, Jr. Rotation of the Andromeda Nebula from a Spectroscopic Survey of Emission Regions. *Astrophys. J.*, 159:379–403, 1970.
- [4] Edwin Hubble and Milton L Humason. The velocity-distance relation among extra-galactic nebulae. *The Astrophysical Journal*, 74:43, 1931.

- [5] Jian Qi Shen. The dark-baryonic matter mass relation for observational... *Gen. Rel. Grav.*, 50(6):73, 2018.
- [6] Mads T. Frandsen and Jonas Petersen. Investigating Dark Matter and MOND Models with Galactic Rotation Curve Data. 2018.
- [7] KG Begeman, AH Broeils, and RH Sanders. Extended rotation curves of spiral galaxies: Dark haloes and modified dynamics. *Monthly Notices of the Royal Astronomical Society*, 249(3):523–537, 1991.
- [8] Stacy McGaugh, Federico Lelli, and Jim Schombert. Radial Acceleration Relation in Rotationally Supported Galaxies. *Phys. Rev. Lett.*, 117(20):201101, 2016.
- [9] Mordehai Milgrom. A modification of the newtonian dynamics as a possible alternative to the hidden mass hypothesis. *The Astrophysical Journal*, 270:365–370, 1983.
- [10] Nathlia Cibirka et al. RELICS: Strong Lensing analysis of the galaxy clusters Abell S295, Abell 697, MACS J0025.4-1222, and MACS J0159.8-0849. 2018.
- [11] Nick Kaiser and Gordon Squires. Mapping the dark matter with weak gravitational lensing. *The Astrophysical Journal*, 404:441–450, 1993.
- [12] M. E. Gray, A. N. Taylor, K. Meisenheimer, S. Dye, C. Wolf, and E. Thommes. Probing the distribution of dark matter in the abell 901/902 supercluster with weak lensing. *Astrophys. J.*, 568:141, 2002.
- [13] Andy N Taylor, DJ Bacon, ME Gray, C Wolf, K Meisenheimer, S Dye, A Borch, M Kleinheinrich, Z Kovacs, and L Wisotzki. Mapping the 3d dark matter with weak lensing in combo-17. *Monthly Notices of the Royal Astronomical Society*, 353(4):1176–1196, 2004.
- [14] J. Ehlers and P. Schneider. Gravitational lensing. In *Proceedings, 13th International Conference on General Relativity and Gravitation: Cordoba, Argentina, June 28-July 4, 1992*, pages 21–40, 1993.
- [15] Douglas Clowe, Maruša Bradač, Anthony H Gonzalez, Maxim Markevitch, Scott W Randall, Christine Jones, and Dennis Zaritsky. A direct empirical proof of the existence of dark matter. *The Astrophysical Journal Letters*, 648(2):L109, 2006.
- [16] Maxim Markevitch, AH Gonzalez, D Clowe, A Vikhlinin, W Forman, C Jones, S Murray, and W Tucker. Direct constraints on the dark matter self-interaction cross section from the merging galaxy cluster 1E 0657-56. *The Astrophysical Journal*, 606(2):819, 2004.
- [17] Maxim Markevitch and Alexey Vikhlinin. Shocks and cold fronts in galaxy clusters. *Physics Reports*, 443(1):1–53, 2007.
- [18] J. R. Brownstein and J. W. Moffat. The Bullet Cluster 1E0657-558 evidence shows Modified Gravity in the absence of Dark Matter. *Mon. Not. Roy. Astron. Soc.*, 382:29–47, 2007.
- [19] Planck Collaboration. Planck 2015 results - xiii. cosmological parameters. *A&A*, 594:A13, 2016.
- [20] Alan H. Guth. The Inflationary Universe: A Possible Solution to the Horizon and Flatness Problems. *Phys. Rev.*, D23:347–356, 1981.
- [21] Andrei D. Linde. The Inflationary Universe. *Rept. Prog. Phys.*, 47:925–986, 1984.
- [22] Andrei D. Linde. A New Inflationary Universe Scenario: A Possible Solution of the Horizon, Flatness, Homogeneity, Isotropy and Primordial Monopole Problems. *Phys. Lett.*, 108B:389–393, 1982.
- [23] Bernard J. Carr. The Origin of Cosmological Density Fluctuations. *Nucl. Phys.*, B252:81–111, 1985.
- [24] Daniel J. Eisenstein et al. Detection of the Baryon Acoustic Peak in the Large-Scale Correlation Function of SDSS Luminous Red Galaxies. *Astrophys. J.*, 633:560–574, 2005.
- [25] P. A. R. Ade et al. Planck 2015 results. XIII. Cosmological parameters. *Astron. Astrophys.*, 594:A13, 2016.
- [26] P. J. E. Peebles and J. T. Yu. Primeval adiabatic perturbation in an expanding universe. *Astrophys. J.*, 162:815–836, 1970.

- [27] J. R. Bond and G. Efstathiou. Cosmic background radiation anisotropies in universes dominated by nonbaryonic dark matter. *Astrophys. J.*, 285:L45–L48, 1984.
- [28] Wayne Hu and Naoshi Sugiyama. Small scale cosmological perturbations: An Analytic approach. *Astrophys. J.*, 471:542–570, 1996.
- [29] Daniel J. Eisenstein and Wayne Hu. Baryonic features in the matter transfer function. *Astrophys. J.*, 496:605, 1998.
- [30] R. F. vom Marttens, L. Casarini, W. S. Hiplito-Ricaldi, and W. Zimdahl. CMB and matter power spectra with non-linear dark-sector interactions. *JCAP*, 1701(01):050, 2017.
- [31] Adam G. Riess, Lucas M. Macri, Samantha L. Hoffmann, Dan Scolnic, Stefano Casertano, Alexei V. Filippenko, Brad E. Tucker, Mark J. Reid, David O. Jones, Jeffrey M. Silverman, Ryan Chornock, Peter Challis, Wenlong Yuan, Peter J. Brown, and Ryan J. Foley. A 2.4% determination of the local value of the hubble constant. *The Astrophysical Journal*, 826(1):56, 2016.
- [32] Wilmar Cardona, Martin Kunz, and Valeria Pettorino. Determining H_0 with Bayesian hyperparameters. *JCAP*, 1703(03):056, 2017.
- [33] Antonio Enea Romano. Hubble trouble or Hubble bubble? 2016.
- [34] Io Oddershov, Steen Hannestad, and Jacob Brandbyge. The variance of the locally measured Hubble parameter explained with different estimators. *JCAP*, 1703(03):022, 2017.
- [35] Richard H. Cyburt, Brian D. Fields, and Keith A. Olive. Primordial nucleosynthesis in light of WMAP. *Phys. Lett.*, B567:227–234, 2003.
- [36] C. Alcock et al. EROS and MACHO combined limits on planetary mass dark matter in the galactic halo. *Astrophys. J.*, 499:L9, 1998.
- [37] M. Davis, G. Efstathiou, C. S. Frenk, and S. D. M. White. The evolution of large-scale structure in a universe dominated by cold dark matter. *apj*, 292:371–394, May 1985.
- [38] Herbert H. Chen. Direct approach to resolve the solar-neutrino problem. *Phys. Rev. Lett.*, 55:1534–1536, Sep 1985.
- [39] Riccardo Barbieri, John Ellis, and Mary K. Gaillard. Neutrino masses and oscillations in su(5). *Physics Letters B*, 90(3):249 – 252, 1980.
- [40] Scott Dodelson and Lawrence M. Widrow. Sterile neutrinos as dark matter. *Phys. Rev. Lett.*, 72:17–20, Jan 1994.
- [41] O. Lahav and A.R. Liddle. The Cosmological Parameters. 21, 2013.
- [42] N. Fornengo. Dark matter overview. In *25th European Cosmic Ray Symposium (ECRS 2016) Turin, Italy, September 04-09, 2016*, 2016.
- [43] R. D. Peccei and Helen R. Quinn. CP conservation in the presence of pseudoparticles. *Phys. Rev. Lett.*, 38:1440–1443, Jun 1977.
- [44] John Preskill, Mark B. Wise, and Frank Wilczek. Cosmology of the invisible axion. *Physics Letters B*, 120(1):127 – 132, 1983.
- [45] Michael Dine and Willy Fischler. The not-so-harmless axion. *Physics Letters B*, 120(1):137 – 141, 1983.
- [46] Joel R. Primack, Jon Holtzman, Anatoly Klypin, and David O. Caldwell. Cold + hot dark matter cosmology with $m(\nu_\mu) \approx m(\nu_\tau) \approx 2.4$ ev. *Phys. Rev. Lett.*, 74:2160–2163, Mar 1995.
- [47] A. Klypin, J. Holtzman, J. Primack, and E. Regos. Structure Formation with Cold plus Hot Dark Matter. *apj*, 416:1, October 1993.
- [48] Scott Dodelson. *Modern Cosmology*. Academic Press, Amsterdam, 2003.
- [49] Carlos S Frenk and Simon DM White. Dark matter and cosmic structure. *Annalen der Physik*, 524(9-10):507–534, 2012.

- [50] J. R. Bond, G. Efstathiou, and J. Silk. Massive Neutrinos and the Large Scale Structure of the Universe. *Phys. Rev. Lett.*, 45:1980–1984, 1980. [,61(1980)].
- [51] J. R. Bond and A. S. Szalay. The Collisionless Damping of Density Fluctuations in an Expanding Universe. *Astrophys. J.*, 274:443–468, 1983.
- [52] Gianfranco Bertone and Dan Hooper. A history of dark matter. *arXiv preprint arXiv:1605.04909*, 2016.
- [53] Marc Davis and P. J. E. Peebles. A Survey of galaxy redshifts. 5. The Two point position and velocity correlations. *Astrophys. J.*, 267:465–482, 1982.
- [54] Erik Holmberg. On the clustering tendencies among the nebulae. ii. a study of encounters between laboratory models of stellar systems by a new integration procedure. *The Astrophysical Journal*, 94:385, 1941.
- [55] Michael Kuhlen, Mark Vogelsberger, and Raul Angulo. Numerical Simulations of the Dark Universe: State of the Art and the Next Decade. *Phys. Dark Univ.*, 1:50–93, 2012.
- [56] Antonio Marrone, Francesco Capozzi, Eleonora Di Valentino, Eligio Lisi, Alessandro Melchiorri, and Antonio Palazzo. Global constraints on neutrino masses and their ordering. *AIP Conf. Proc.*, 1894(1):020015, 2017.
- [57] Carlos S. Frenk, Simon D. M. White, and Marc Davis. Nonlinear evolution of large-scale structure in the universe. *Astrophys. J.*, 271:417, 1983.
- [58] Ya. B. Zeldovich, J. Einasto, and S. F. Shandarin. Giant Voids in the Universe. *Nature*, 300:407–413, 1982.
- [59] A Dekel and SJ Aarseth. The spatial correlation function of galaxies confronted with theoretical scenarios. *The Astrophysical Journal*, 283:1–23, 1984.
- [60] Simon DM White, CS Frenk, and Marc Davis. Clustering in a neutrino-dominated universe. *The Astrophysical Journal*, 274:L1–L5, 1983.
- [61] John Huchra, Marc Davis, David Latham, and J Tonry. A survey of galaxy redshifts. iv-the data. *The Astrophysical Journal Supplement Series*, 52:89–119, 1983.
- [62] PR Shapiro, C Struck-Marcell, and AL Melott. Pancakes and the formation of galaxies in a neutrino-dominated universe. *The Astrophysical Journal*, 275:413–429, 1983.
- [63] YA B Zel'Dovich. Gravitational instability: An approximate theory for large density perturbations. *Astronomy and astrophysics*, 5:84–89, 1970.
- [64] Matthew R. Buckley and Annika H. G. Peter. Gravitational probes of dark matter physics. 2017.
- [65] James S. Bullock and Michael Boylan-Kolchin. Small-Scale Challenges to the Λ CDM Paradigm. *Ann. Rev. Astron. Astrophys.*, 55:343–387, 2017.
- [66] Julio F Navarro, Carlos S Frenk, and Simon DM White. A universal density profile from hierarchical clustering. *The Astrophysical Journal*, 490(2):493, 1997.
- [67] Julio F. Navarro, Aaron Ludlow, Volker Springel, Jie Wang, Mark Vogelsberger, Simon D. M. White, Adrian Jenkins, Carlos S. Frenk, and Amina Helmi. The Diversity and Similarity of Cold Dark Matter Halos. *Mon. Not. Roy. Astron. Soc.*, 402:21, 2010.
- [68] R Brent Tully and J Richard Fisher. A new method of determining distances to galaxies. *Astronomy and Astrophysics*, 54:661–673, 1977.
- [69] Andrey V. Kravtsov. The size - virial radius relation of galaxies. *Astrophys. J.*, 764:L31, 2013.
- [70] Fabio Governato et al. At the heart of the matter: the origin of bulgeless dwarf galaxies and Dark Matter cores. *Nature*, 463:203–206, 2010.
- [71] Mei-Yu Wang, Louis E. Strigari, Mark R. Lovell, Carlos S. Frenk, and Andrew R. Zentner. Mass assembly history and infall time of the Fornax dwarf spheroidal galaxy. *Mon. Not. Roy. Astron. Soc.*, 457(4):4248–4261, 2016.

- [72] Oleg Y. Gnedin, Daniel Ceverino, Nickolay Y. Gnedin, Anatoly A. Klypin, Andrey V. Kravtsov, Robyn Levine, Daisuke Nagai, and Gustavo Yepes. Halo Contraction Effect in Hydrodynamic Simulations of Galaxy Formation. 2011.
- [73] Andrea V. Maccio', Greg Stinson, Chris B. Brook, James Wadsley, H. M. P. Couchman, Sijing Shen, Brad K. Gibson, and Tom Quinn. Halo expansion in cosmological hydro simulations: towards a baryonic solution of the cusp/core problem in massive spirals. *Astrophys. J.*, 744:L9, 2012.
- [74] S. Courteau, A. A. a Dutton, F. van den Bosch, L. A. MacArthur, A. Dekel, D. H. McIntosh, and Daniel A. Dale. Scaling Relations of Spiral Galaxies. *Astrophys. J.*, 671:203, 2007.
- [75] Aaron A. Dutton, Charlie Conroy, Frank C. van den Bosch, Luc Simard, Trevor Mendel, Stephane Courteau, Avishai Dekel, Surhud More, and Francisco Prada. Dark halo response and the stellar initial mass function in early-type and late-type galaxies. *Mon. Not. Roy. Astron. Soc.*, 416:322, 2011.
- [76] Sergey Mashchenko, H. M. P. Couchman, and James Wadsley. Cosmological puzzle resolved by stellar feedback in high redshift galaxies. *Nature*, 442:539, 2006.
- [77] Sergey Mashchenko, James Wadsley, and H. M. P. Couchman. Stellar Feedback in Dwarf Galaxy Formation. *Science*, 319:174, 2008.
- [78] Andrew Pontzen and Fabio Governato. How supernova feedback turns dark matter cusps into cores. *Mon. Not. Roy. Astron. Soc.*, 421:3464, 2012.
- [79] Arnab Rai Choudhuri. *The Physics of Fluids and Plasmas: An Introduction for Astrophysicists*. Cambridge University Press, 1998.
- [80] Hua bai Li and Thomas Henning. The alignment of molecular cloud magnetic fields with the spiral arms in m33. *Nature*, 479:499–501, 2011.
- [81] Peter J. Cossins. Smoothed Particle Hydrodynamics. 2010.
- [82] J. J. Monaghan. Smoothed particle hydrodynamics. *Annual Review of Astronomy and Astrophysics*, 30(1):543–574, 1992.
- [83] N. Y. Gnedin. Softened Lagrangian hydrodynamics for cosmology. *apjs*, 97:231–257, April 1995.
- [84] G. J. Ferland, K. T. Korista, D. A. Verner, J. W. Ferguson, J. B. Kingdon, and E. M. Verner. Cloudy 90: Numerical simulation of plasmas and their spectra. *Publications of the Astronomical Society of the Pacific*, 110(749):761, 1998.
- [85] M. Schmidt. The Rate of Star Formation. *apj*, 129:243, March 1959.
- [86] Mark R. Krumholz and Jonathan C. Tan. Slow star formation in dense gas: Evidence and implications. *The Astrophysical Journal*, 654(1):304, 2007.
- [87] J. Guedes, S. Callegari, P. Madau, and L. Mayer. Forming Realistic Late-type Spirals in a Λ CDM Universe: The Eris Simulation. *apj*, 742:76, December 2011.
- [88] R. Klement, B. Fuchs, and H.-W. Rix. Identifying stellar streams in the first rave public data release. *The Astrophysical Journal*, 685(1):261, 2008.
- [89] Michael Odenkirchen, Eva K. Grebel, Constance M. Rockosi, Walter Dehnen, Rodrigo Ibata, Hans-Walter Rix, Andrea Stolte, Christian Wolf, Jr. John E. Anderson, Neta A. Bahcall, Jon Brinkmann, Istvn Csabai, G. Hennessy, Robert B. Hindsley, eljko Ivezi, Robert H. Lupton, Jeffrey A. Munn, Jeffrey R. Pier, Chris Stoughton, and Donald G. York. Detection of massive tidal tails around the globular cluster palomar 5 with Sloan Digital Sky Survey commissioning data. *The Astrophysical Journal Letters*, 548(2):L165, 2001.
- [90] Nilanjan Banik, Gianfranco Bertone, Jo Bovy, and Nassim Bozorgnia. Probing the nature of dark matter particles with stellar streams. 04 2018.
- [91] Denis Erkal, Sergey E. Koposov, and Vasily Belokurov. A sharper view of pal 5's tails: discovery of stream perturbations with a novel non-parametric technique. *Monthly Notices of the Royal Astronomical Society*, 470(1):60–84, 2017.

- [92] David N. Spergel and Paul J. Steinhardt. Observational evidence for selfinteracting cold dark matter. *Phys. Rev. Lett.*, 84:3760–3763, 2000.
- [93] Annika H. G. Peter, Miguel Rocha, James S. Bullock, and Manoj Kaplinghat. Cosmological Simulations with Self-Interacting Dark Matter II: Halo Shapes vs. Observations. *Mon. Not. Roy. Astron. Soc.*, 430:105, 2013.
- [94] Miguel Rocha, Annika H. G. Peter, James S. Bullock, Manoj Kaplinghat, Shea Garrison-Kimmel, Jose Onorbe, and Leonidas A. Moustakas. Cosmological Simulations with Self-Interacting Dark Matter I: Constant Density Cores and Substructure. *Mon. Not. Roy. Astron. Soc.*, 430:81–104, 2013.
- [95] Wayne Hu, Rennan Barkana, and Andrei Gruzinov. Cold and fuzzy dark matter. *Phys. Rev. Lett.*, 85:1158–1161, 2000.
- [96] M. Nori and M. Baldi. AX-GADGET: a new code for cosmological simulations of Fuzzy Dark Matter and Axion models. 2018.
- [97] Vid Iri, Matteo Viel, Martin G. Haehnelt, James S. Bolton, and George D. Becker. First constraints on fuzzy dark matter from Lyman- α forest data and hydrodynamical simulations. *Phys. Rev. Lett.*, 119(3):031302, 2017.
- [98] Mark R. Lovell, Carlos S. Frenk, Vincent R. Eke, Adrian Jenkins, Liang Gao, and Tom Theuns. The properties of warm dark matter haloes. *Mon. Not. Roy. Astron. Soc.*, 439:300–317, 2014.
- [99] Alexey Boyarsky, Oleg Ruchayskiy, and Mikhail Shaposhnikov. The Role of sterile neutrinos in cosmology and astrophysics. *Ann. Rev. Nucl. Part. Sci.*, 59:191–214, 2009.
- [100] E. Komatsu et al. Seven-Year Wilkinson Microwave Anisotropy Probe (WMAP) Observations: Cosmological Interpretation. *Astrophys. J. Suppl.*, 192:18, 2011.
- [101] Mark R. Lovell, Vincent Eke, Carlos S. Frenk, Liang Gao, Adrian Jenkins, Tom Theuns, Jie Wang, D. M. White, Alexey Boyarsky, and Oleg Ruchayskiy. The Haloes of Bright Satellite Galaxies in a Warm Dark Matter Universe. *Mon. Not. Roy. Astron. Soc.*, 420:2318–2324, 2012.
- [102] Andrea V. Maccio, Sinziana Paduroiu, Donnino Anderhalden, Aurel Schneider, and Ben Moore. Cores in warm dark matter haloes: a Catch 22 problem. *Mon. Not. Roy. Astron. Soc.*, 424:1105–1112, 2012.
- [103] Benoit Famaey and Stacy McGaugh. Modified Newtonian Dynamics (MOND): Observational Phenomenology and Relativistic Extensions. *Living Rev. Rel.*, 15:10, 2012.
- [104] Mordehai Milgrom. MOND-theoretical aspects. *New Astron. Rev.*, 46:741–753, 2002.
- [105] Paul M. Chesler and Abraham Loeb. Constraining Relativistic Generalizations of Modified Newtonian Dynamics with Gravitational Waves. *Phys. Rev. Lett.*, 119(3):031102, 2017.
- [106] Jacob D. Bekenstein. Relativistic gravitation theory for the MOND paradigm. *Phys. Rev.*, D70:083509, 2004. [Erratum: Phys. Rev.D71,069901(2005)].
- [107] Constantinos Skordis, D. F. Mota, P. G. Ferreira, and C. Boehm. Large Scale Structure in Bekenstein’s theory of relativistic Modified Newtonian Dynamics. *Phys. Rev. Lett.*, 96:011301, 2006.
- [108] Constantinos Skordis. The Tensor-Vector-Scalar theory and its cosmology. *Class. Quant. Grav.*, 26:143001, 2009.
- [109] B.P. Abbott et al. GW170817: Observation of Gravitational Waves from a Binary Neutron Star Inspiral. *Phys. Rev. Lett.*, 119(16):161101, 2017.
- [110] S. Boran, S. Desai, E. O. Kahya, and R. P. Woodard. GW170817 Falsifies Dark Matter Emulators. *Phys. Rev.*, D97(4):041501, 2018.
- [111] Irwin I. Shapiro. Fourth Test of General Relativity. *Phys. Rev. Lett.*, 13:789–791, 1964.
- [112] Guy D. Moore and Ann E. Nelson. Lower bound on the propagation speed of gravity from gravitational Cherenkov radiation. *JHEP*, 09:023, 2001.

- [113] Joshua W. Elliott, Guy D. Moore, and Horace Stoica. Constraining the new Aether: Gravitational Cerenkov radiation. *JHEP*, 08:066, 2005.
- [114] B. P. Abbott et al. Observation of Gravitational Waves from a Binary Black Hole Merger. *Phys. Rev. Lett.*, 116(6):061102, 2016.
- [115] Craig Lage and Glennys R Farrar. The bullet cluster is not a cosmological anomaly. *Journal of Cosmology and Astroparticle Physics*, 2015(02):038, 2015.
- [116] Garry W Angus, Huan Yuan Shan, Hong Sheng Zhao, and Benoit Famaey. On the proof of dark matter, the law of gravity, and the mass of neutrinos. *The Astrophysical Journal Letters*, 654(1):L13, 2006.
- [117] Zhe Chang, Ming-Hua Li, Xin Li, Hai-Nan Lin, and Sai Wang. Finslerian MOND versus the Strong Gravitational Lensing of the Early-type Galaxies. *Eur. Phys. J.*, C73:2550, 2013.
- [118] Stacy S. McGaugh. A Novel Test of the Modified Newtonian Dynamics with Gas Rich Galaxies. *Phys. Rev. Lett.*, 106:121303, 2011. [Erratum: *Phys. Rev. Lett.* 107, 229901 (2011)].
- [119] Xin Li, Ming-Hua Li, Hai-Nan Lin, and Zhe Chang. Finslerian MOND vs. observations of Bullet Cluster 1E0657-558. *Mon. Not. Roy. Astron. Soc.*, 428(4):2939–2948, 2013.
- [120] Zhe Chang, Ming-Hua Li, Xin Li, Hai-Nan Lin, and Sai Wang. Effects of spacetime anisotropy on the galaxy rotation curves. *Eur. Phys. J.*, C73:2447, 2013.